

https://dspace.org/

# Lipase-catalysed hydrolysis of morita-baylis-hillman adducts

**Mguni, Lindelo Mthabisi**

**2019**

https://hdl.handle.net/10539/29664

Mguni,Lindelo Mthabisi (2019) Lipase-catalysed hydrolysis of Morita-Baylis-Hillman adducts, University of the Witwatersrand, Johannesburg, <http://hdl.handle.net/10539/29664>

Downloaded from a DSpace repository. https://dspace.org/




# LIPASE-CATALYSED HYDROLYSIS OF MORITA-BAYLIS-HILLMAN ADDUCTS

by

**Lindelo Mthabisi Mguni**

**1793430**

A dissertation

Submitted in fulfilment of the requirements for the degree

**Master of Science**

in

**Molecular and Cell Biology**

in the Faculty of Science, University of the Witwatersrand, Johannesburg, South Africa

Supervisor: Professor Karl Rumbold

Co-supervisor: Professor Moira Bode

June 2019

# DECLARATION

I, Lindelo Mthabisi Mguni (1793430), am a student registered for the degree of Master of Science by Research in the academic year 2019.

I hereby declare the following:

- I am aware that plagiarism (the use of someone else's work without their permission and/or without acknowledging the original source) is wrong.
- I confirm that the research proposal submitted for assessment for the above degree is my own unaided work except where explicitly indicated otherwise and acknowledged.
- I have followed the required conventions in referencing the thoughts and ideas of others.
- I understand that the University of the Witwatersrand may take disciplinary action against me if there is a belief that this is not my own unaided work or that I have
- failed to acknowledge the source of the ideas or words in my writing.

Signature:  24th day of June 2019

# ABSTRACT

Biocatalysis is the use of biological systems, such as enzymes, to perform chemical transformations on organic compounds. These enzymes catalyse reactions as whole cell systems or in isolated forms and have been found to exhibit high regio- and stereoselectivity towards chiral compounds. Lipases have been extensively used to catalyse kinetic resolutions of chiral compounds such as the Morita-Baylis-Hillman (MBH) adducts. The MBH adducts and their esters are important intermediates in organic synthesis and have been found to be valuable in the production of biologically active compounds. In this study, we expressed and partially purified the *Pseudomonas fluorescens* P26504 lipase in an active and soluble form to catalyse the kinetic resolution on MBH acetates to obtain enantiopure MBH adducts. The *Pseudomonas fluorescens* P26504 lipase was overexpressed in BL21 (DE3) pLysS cells at 25 °C for 16 hours, with 1mM IPTG concentration. Enzymatic assays were conducted after partial purification using *p*-nitrophenyl esters. The recombinant enzyme was highly active towards short chain esters and showed moderate activity towards medium chained esters. The Morita-Baylis-Hillman reaction was conducted, giving rise to racemic MBH adducts derived from benzaldehyde and hydro-cinnamaldehyde. The second step of the reaction was acetylation, producing chiral MBH acetates. A lipase-catalysed kinetic resolution was set-up, using the partially purified recombinant *P. fluorescens* P26504 lipase and the MBH acetates. TLC plate analysis showed that the recombinant lipase was able to hydrolyse both MBH acetates. However, further studies can be done to determine the enantioselectivity of the recombinant *P. fluorescens* P26504 lipase using chiral HPLC, which is more definitive.

I dedicate this thesis to my mother

❖

Sithembiso Mguni

*‘Ad Definitum Finem’*

# ACKNOWLEDGEMENTS

I would like to thank my supervisor Professor Karl Rumbold, for granting me this opportunity by accepting me in his lab, his support and guidance throughout. It felt at home.

I would also like to extend my thanks to my co-supervisor Professor Moira L. Bode, who was of huge assistance in my exploration of the organic chemistry world. I am forever grateful.

I would also like to thank Dr Charles Changunda, who assisted with the NMR analysis and words of encouragement, and Selisha A. Sooklal with the insight in protein purification.

A special thanks to my family, particularly my mother, Mrs Sithembiso Mguni, Mr Simon Mberi and Mrs Debrah Mberi for the financial support throughout, their love and words of encouragement.

Above all, I thank the Lord All Mighty for taking me this far. He is Jehovah Ra-ah (The Lord my shepherd).

# CONTENTS

**DECLARATION** ..... i
**ABSTRACT** ..... ii
**ACKNOWLEDGEMENTS** ..... iv
**LIST OF FIGURES** ..... vii
**LIST OF SCHEMES** ..... x
**LIST OF TABLES** ..... xi
**1 LITERATURE REVIEW** ..... 1
**1.1 Biocatalysis** ..... 1
**1.2 Lipases** ..... 2
**1.2.1 Lipase Structure and Function** ..... 3
**1.2.2 Properties of *Pseudomonas* lipases** ..... 5
**1.2.3 Expression and Purification of *Pseudomonas* Lipases** ..... 10
**1.2.4 Industrial Uses of Lipases** ..... 12
**1.3 Morita-Baylis-Hillman Reaction** ..... 14
**1.3.1 Lipase-Catalysed Kinetic Resolutions of MBHAs** ..... 16
**1.4 RATIONALE** ..... 17
**2 AIM AND OBJECTIVES** ..... 18
**2.1 Aim** ..... 18
**2.2 Objectives** ..... 18
**3 METHODS AND MATERIALS** ..... 19
**3.1 Preparation of competent cells** ..... 19
**3.2 Transformation** ..... 19
**3.3 Plasmid Extraction and Confirmation** ..... 20
**3.3.1 Restriction Digest** ..... 20
**3.3.2 Agarose Gel Electrophoresis Confirmation** ..... 21
**3.4 Expression Trials** ..... 21
**3.4.1 Sodium Dodecyl Sulfate-Polyacrylamide Gel Electrophoresis (SDS-PAGE)** ..... 22
**3.5 Over-expression and Purification** ..... 24
**3.6. Enzyme Assay** ..... 24
**3.7 Morita-Baylis-Hillman Reaction** ..... 25
**3.7.1 Column Chromatography** ..... 26
**3.7.2 Synthesis of (±)-2-[(hydroxyphenyl)methyl]acrylonitrile 10a** ..... 27
**3.7.3 Synthesis of (±)-2-cyano-1-phenylallyl acetate 11a** ..... 27
**3.7.4 Synthesis of (±)-3-hydroxy-2-methylene-5-phenylpentanenitrile 10b** ..... 27

**3.7.5 Synthesis of (±)-2-cyano-5-phenyl-pent-1-ene-yl acetate 11b** ..... 27
**3.8 Enzymatic Hydrolysis of Morita-Baylis-Hillman acetates** ..... 28
**4 RESULTS** ..... 29
**4.1 Transformation** ..... 29
**4.2 Expression Trials** ..... 30
**4.3 Overexpression and Partial Purification** ..... 32
**4.4 Enzyme Assays** ..... 34
**4.5 Morita-Baylis-Hillman Adducts** ..... 36
**4.5.1 Synthesis of (±)-2-cyano-1-phenylallyl acetate 11a** ..... 36
**4.5.2 Synthesis of (±)-2-cyano-5-phenyl-pent-1-ene-yl-acetate 11b** ..... 36
**4.6 Enzymatic Hydrolysis** ..... 36
**5 DISCUSSION** ..... 40
**5.1 Transformation** ..... 40
**5.2 Expression Trials and Overexpression** ..... 41
**5.3 Partial Purification** ..... 42
**5.4 Enzyme assays** ..... 43
**5.5 Morita-Baylis-Hillman Reaction** ..... 43
**5.5.1 Preparation of Morita-Baylis-Hillman adducts 10a and 10b** ..... 44
**5.5.2 Preparation of Morita-Baylis-Hillman acetates 11a and 11b** ..... 44
**5.6 Lipase Catalysed Kinetic Resolution** ..... 45
**6 CONCLUSIONS** ..... 47
**6.1 Recommendations** ..... 48
**7 REFERENCES** ..... 49
**Appendix** ..... 58
**A1 Molecular Weight Ladders** ..... 58
**A2 Standard Curve Data** ..... 60
**A3 NMR Spectrums** ..... 62

# LIST OF FIGURES

**Figure 1. 1** Catalytic action of Lipases. Hydrolysis occurs in water-lipid interface catalysing a triacylglycerol into glycerol and fatty acids. .....3

**Figure 1. 2.** Schematic overview of the α/β- hydrolase fold. The α-helices are indicated by bars and β-sheets by arrows. X represents the active site residue positions. N = amino-terminal, C = carboxyl-terminal (Holmquist, 2000). .....4

**Figure 1. 3.** Lipase Hydrolysis Mechanism of an Ester Bond (Holmquist, 2000). .....5

**Figure 1. 4:** Secondary alcohol consisting of two substituents of different sizes. L represents the large substituent and M a medium-sized substituent. .....9

**Figure 1. 5**: Various Industrial Applications of Lipases (Angajala *et al*., 2016) .....12

**Figure 1. 6**: Morita-Baylis-Hillman reaction (Juma *et al*., 2017) .....14

**Figure 1. 7**: MBH reaction with a wide variety of activated alkenes. Reaction is conducted with aldehydes at atmospheric pressure and DABCO catalyst. .....16

**Figure 4. 1**: Agarose gel electrophoresis of extracted pET11a plasmid from JM109 cells. An aliquot of 5 µl of the restriction digest samples were loaded on the gel. MW represented the molecular weight marker 1 Kb. On lane 2, undigested plasmid was loaded; lane 3 was loaded with BamHI digested plasmid; lane 4 with NdeI digested plasmid and lane 5 with double digested plasmid (BamHI and NdeI). Plasmid size = 5675 bp; Gene of interest size = 1359 bp. .....29

**Figure 4. 2:** Agarose gel electrophoresis of extracted pET11a plasmid from BL21 (DE3) pLysS cells. An aliquot of 5 µl of the restriction digest samples were loaded on the gel. MW represented the molecular weight marker 1 Kb. On lane 1, undigested plasmid was loaded; lane 2 was loaded with BamHI digested plasmid; lane 3 with NdeI digested plasmid and lane 4 with double digested plasmid (BamHI and NdeI). Plasmid size = 5675 bp; Gene of interest size = 1359 bp. .....30

**Figure 4. 3:** SDS-PAGE analysis of the expression trial at 25 °C. The pET11a plasmid containing the *Pseudomonas fluorescens* lipase gene expressed in *E. coli* BL21 (DE3) pLySs. MW represents the PageRuler Unstained Protein Ladder(10-200kDa), P represent the resuspended pellet and S represents the supernatant. The protein (48.2 kDa) was not expressed at 4 hours. Protein expression in a soluble form seen from 8 hours to 16 hours, with high expression at 1mM IPTG concentration. (as shown in the red box). .....31

**Figure 4. 4:** SDS-PAGE analysis of the expression trial at 30 °C. The pET11a plasmid containing the *Pseudomonas fluorescens* lipase gene expressed in *E. coli* BL21 (DE3) pLySs. MW represents the PageRuler Unstained Protein Ladder(10-200kDa), P represent the resuspended pellet and S represents the supernatant. The protein (48.2 kDa) was not expressed at 4 hours. Protein expression in a soluble form seen from 8 hours to 16 hours,

with high expression at 1mM IPTG concentration. At 24 hours, it was insoluble (as shown in the red box).....31

**Figure 4. 5:** SDS-PAGE analysis of the expression trial at 37 °C. The pET11a plasmid containing the *Pseudomonas fluorescens* lipase gene expressed in *E. coli* BL21 (DE3) pLySs. MW represents the PageRuler Unstained Protein Ladder(10-200kDa), P represent the resuspended pellet and S represents the supernatant. High expression in the supernatant seen at 4 hours and 8 hours. Expression at 12 hours was in the pellet form. Protein indicated as dark bands at close to 50 kDa mark (as shown in the red box).....32

**Figure 4. 6:** Elution chromatogram of the recombinant *Pseudomonas fluorescens* lipase. The blue line represents absorbance of the supernatant, orange represents conductivity and the grey line represents the salt concentration at a linear gradient.....33

**Figure 4. 7:** SDS-PAGE analysis of the lipase expressed in *E. coli* and purified on the Akta Prime Plus using the HiTrap DEAE Sepharose FF column. MW represents the PageRuler Unstained Protein Ladder, P represents the resuspended pellet after sonication (with presence of protein in the red box), C represents the supernatant after sonication and centrifugation (also referred to as the crude), FT represents the flow through during purification, W represents the column wash after binding the protein to the column and numbers 1 to 10 are the different fractions collect with number 7 and 8 showing where the protein eluted (red box). The size of the lipase was 48.2 kDa. .....34

**Figure 4. 8:** Standard curve used to determine the rPFL activity based on the amount of *p*-nitrophenol liberated during the reaction.....35

**Figure 4. 9:** TLC plate under UV showing the hydrolysis of the substrate (±)-2-cyano-1-phenyl allyl acetate **11a**. Spot number 1 represents the starting material **10a**; spot number 2 represents the alcohol derivative, **10a**; spot number 3 represents the substrate hydrolysed by the crude enzyme extract; spot 4 is the substrate with crude enzyme extract with calcium ions; spot 5 represents the substrate hydrolysed by the recombinant *P. fluorescens* lipase in the presence of calcium ions and spot 6 represents hydrolysis of the substrate by the recombinant *P. fluorescens* with no calcium ions. Highlighted in Red are the spots corresponding to the starting material and in Yellow corresponding to the alcohol derivative. .....38

**Figure 4. 10:** TLC plate under UV showing the hydrolysis of the substrate (±)-2-cyano-5-phenyl-pent-1-ene-yl acetate **11b**. Spot number 1 represents the starting material **11b** and a faint spot for product **10b**; spot number 2 represents the substrate hydrolysed by the crude enzyme extract with calcium ions; spot 3 is the substrate with crude enzyme extract; spot 4 represents the substrate hydrolysed by the recombinant *P. fluorescens* lipase in the presence of calcium ions and spot 5 represents hydrolysis of the substrate by the recombinant *P. fluorescens* lipase with no calcium ions. Highlighted in Red are the spots corresponding to the starting material and in Yellow corresponding to the alcohol derivative. .....39

**Figure A1. 1**: 1KB DNA Ladder used for agarose gel electrophoresis .....58
**Figure A1. 2**: PageRuler Unstained Protein Ladder for SDS-PAGE analysis.....59

**Figure A3. 1**: $^{1}$H NMR spectra for **11a**.....62
**Figure A3. 2**: $^{13}$C NMR spectra for **11a**.....63
**Figure A3. 3**: $^{1}$H NMR spectra for **11b**.....64
**Figure A3. 4**: $^{13}$C NMR spectra for **11b**.....65

# LIST OF SCHEMES

**Scheme 1. 1**: Generally accepted MBH reaction mechanism .....15

**Scheme 3. 1**: Preparation of Morita-Baylis-Hillman adducts **10** and acetates **11**. The aldehyde (**8**) is mixed with acrylonitrile (**9**) and the reaction is catalysed by DABCO (**1**). Acetylation is done using triethylamine and acetic anhydride.....26

**Scheme 4. 1**: Enzymatic hydrolysis of Morita-Baylis-Hillman acetates.....37

# LIST OF TABLES

**Table 1. 1:** Properties of *Pseudomonas* lipases in literature. .....7

**Table 3. 1:** Electrode and gel stock solutions for SDS-PAGE.....23

**Table 4. 1:** Lipase activity measured using *p*-nitrophenyl esters. .....35

**Table A2. 1**: Standard curve data .....60

**Table A2. 2**: Standard curve data 2, showing Standard deviation .....61

# 1 LITERATURE REVIEW

## 1.1 Biocatalysis

Some chemical reactions occur spontaneously whilst other reactions require catalysis for them to proceed at a significant rate. Catalysts are compounds that reduce the magnitude of the energy barrier required for the conversion of one chemical substance into another. Industrial synthetic chemistry uses catalytic processes in the synthesis of approximately 80 – 90 % of products (Shaikh, 2014). Most chemical catalysts used are in the form of metals and oxides, nevertheless, some of those have been found to create undesirable toxic by-products. The development of green chemistry has been efficient as it utilizes renewable raw materials and eliminates waste and these toxic by-products. This in-turn has led to the prolific use of biocatalysts in organic synthesis (Drauz *et al*., 2012; Sheldon *et al*., 2007 ).

Biocatalysis is the transformation of substances of chemical or biological origin using biological (living) systems or their components. On an industrial scale, biocatalsysts applied in different processes for catalysis are either proteins (enzymes) or, in a few cases, nucleic acids such as ribozymes (Mateo and Palomo, 2018). Enzymes have been found to catalyse these reactions either as whole cells systems or in isolated forms. Isolated enzymes, purified and concentrated, have been used to a greater extent compared to whole cell systems because they produce cleaner products. This is due to the presence of other cell components in whole cells hence an interference or dominance of unwanted side reactions rendering by-products. Enzyme application as biocatalysts in synthetic organic chemistry has increased due to their high regio- and stereoselectivity required for the creation of chiral compounds. This in-turn has led to a decrease in the use of downstream processes (Davids *et al*., 2013).The use of enzymes also fulfils the central principles of green chemistry as they are biodegradable and produced from inexpensive renewable resources, hence offering environmental and economic advantages as compared to chemical catalysts (Truppo, 2017).

Biocatalysts have drawbacks such as low stability in desired media as they denature at extremes of temperature and pH, biocatalytic pathways taking longer to establish and also very few biocatalysts exist for desired reactions from available substrates to targeted products (Bommarius and Riebel, 2004). Biotechnological techniques such as protein engineering, enzyme screening and enzyme immobilisation have been used to overcome drawbacks of

enzymes in synthetic chemistry. Protein engineering is mainly used focusing on enzymatic activity with a goal of enhancing substrate specificity and enantioselectivity. Directed evolution approaches have mainly been used in optimising the rate of the biocatalyst (Bezborodov and Zagustina, 2014; Macrae and Hammond, 2013).

Among industrial enzymes used in organic synthesis, lipases have been found to be the most promising enzymes for broad practical application. Lipases are the most frequently used enzymes in this area particularly because the control of stereochemistry is important. Research on these enzymes has extensively been based on their structural elucidation, mechanism of action, performance characterisation and, sequencing and cloning (Alberghina, 1991).

## 1.2 Lipases

Lipases, triacylglycerol ester hydrolases (EC 3.1.1.3), are enzymes that catalyse the hydrolysis of triglycerides to diacylglycerol, monoacylglycerol and glycerol and free fatty acids (Figure 1.1). They differ from esterases (EC 3.1.1.1), which only act on water-soluble carboxylic ester molecules, by conducting this hydrolytic reaction at a water-lipid interface and reversing the reaction in a non-aqueous environment (Lasoń and Ogonowski, 2010). In the reverse reaction, the enzyme is able to synthesise new molecules by esterification, alcoholysis and transesterification (Ghori *et al.*, 2011).

Lipases are ubiquitous in nature and are widely distributed in animals, plants and microorganisms. They have a molecular weight range of between 20 and 70 kDa, optimum pH activity range of 4 - 9 and a temperature range between 25 – 70 °C. They differ greatly in respect to both their origins and their properties, for example, with regards to positional specificity, thermostability and pH optimum (Hasan *et al.*, 2006; Thakur, 2012). Microbial lipases have been extensively used since they are stable in organic solvents and exhibit high enantioselectivity as compared to the other lipases from other sources. Microbial lipases also possess a broad substrate specificity and do not require cofactors to activate them. Studies conducted on lipases have contributed to the elucidation of the structure-function relationships, hence bringing apprehension of the kinetic mechanisms of lipase action (Jaeger and Reetz, 1998; Saxena *et al*., 2003).

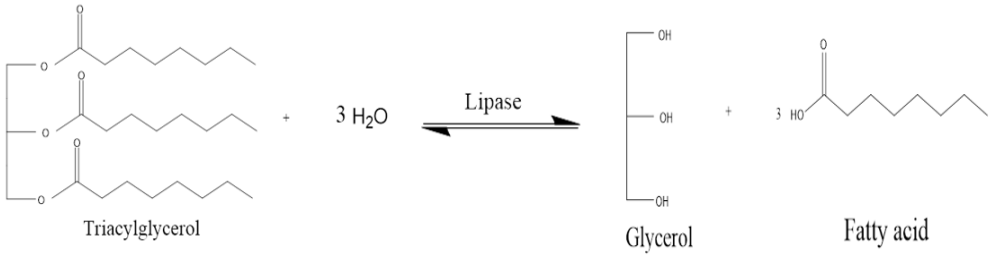



**Figure 1. 1** Catalytic action of Lipases. Hydrolysis occurs in water-lipid interface catalysing a triacylglycerol into glycerol and fatty acids.

## 1.2.1 Lipase Structure and Function

The increasing demand for microbial lipases in organic synthesis has led to the evaluation of their catalytic activity and their unique properties that enable them to function in non-aqueous environments (Stoytcheva *et al.*, 2012). They were found to show a typical folding pattern referred to as the α/β- hydrolase fold (Bell *et al.*, 2002). The lipase core is made up of a central β sheet consisting of eight different β strands (β1-β8) connected to six α strands (αA-αF) with two hinge segments on both of its ends (Figure 1.2). These hydrolases have an active site that contains a catalytic triad made up of a nucleophilic serine, aspartic/glutamic acid and a histidine residue, and usually also a consensus sequence (Gly-$X_1$-Ser-$X_2$-Gly) is found around the serine (Jaeger *et al.*, 1999).

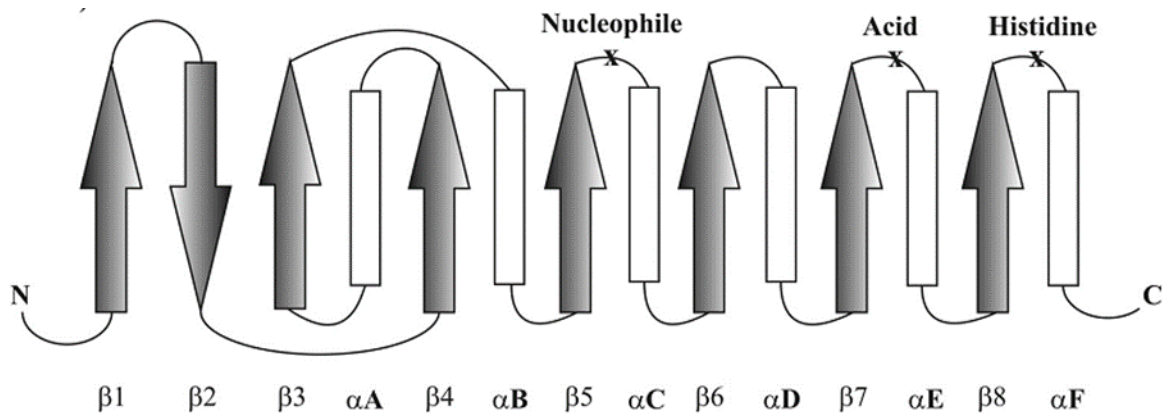



**Figure 1. 2.** Schematic overview of the α/β- hydrolase fold. The α-helices are indicated by bars and β-sheets by arrows. X represents the active site residue positions. N = amino-terminal, C = carboxyl-terminal (Holmquist, 2000).

The active site of a lipase has been found to be shielded by a lid-like alpha-helical oligopeptide unit and this conserved form plays a role in the stability of the enzyme in organic solvents (Bornscheuer *et al*., 2002). The alpha-helical oligopeptide is amphiphilic in nature and its flexible conformation determines the state of the enzyme. It can adopt an inactive state, referred to as a closed conformation, in which the active-site is covered by the lid, and an active state, or open conformation, in which the substrate gains full access to the active site (Ferrario *et al.*, 2011). The alpha-helical oligopeptide unit undergoes sequential changes when in contact with the substrate of the lipase, thus exposing the hydrophobic residues at the enzyme's active site. This phenomenon is known as interfacial activation (Anjagala *et al.*, 2016; Jaeger *et al.*, 1994).

Substrate hydrolysis is initiated by a nucleophilic attack on the carbonyl carbon of an ester bond by the catalytic site serine residue which is found on the C-terminal end of the central β5 strand generating a negatively charged tetrahedral intermediate (Sarmah *et al*., 2018). This intermediate is stabilized by hydrogen bonding between the oxygen and protons attached to nitrogen atoms of main-chain residues belonging to what is called the oxyanion hole. Nucleophilicity of the attacking serine oxygen is enhanced by hydrogen bonding of the OH to an adjacent histidine nitrogen. Electrons in the oxyanion are then pushed back to the carbonyl carbon, releasing an alcohol. The next step is hydrolysis of the acyl-enzyme complex by a water molecule. The nucleophilicity of the water oxygen atom is enhanced by hydrogen-bonding to a histidine nitrogen atom. The acyl-lipase complex is then hydrolysed by nucleophilic attack of the water oxygen atom, forming another tetrahedral intermediate that then collapses and

liberates a fatty acid and regenerates the enzyme as shown in Figure 1.3 (Jaeger and Reetz, 1998).

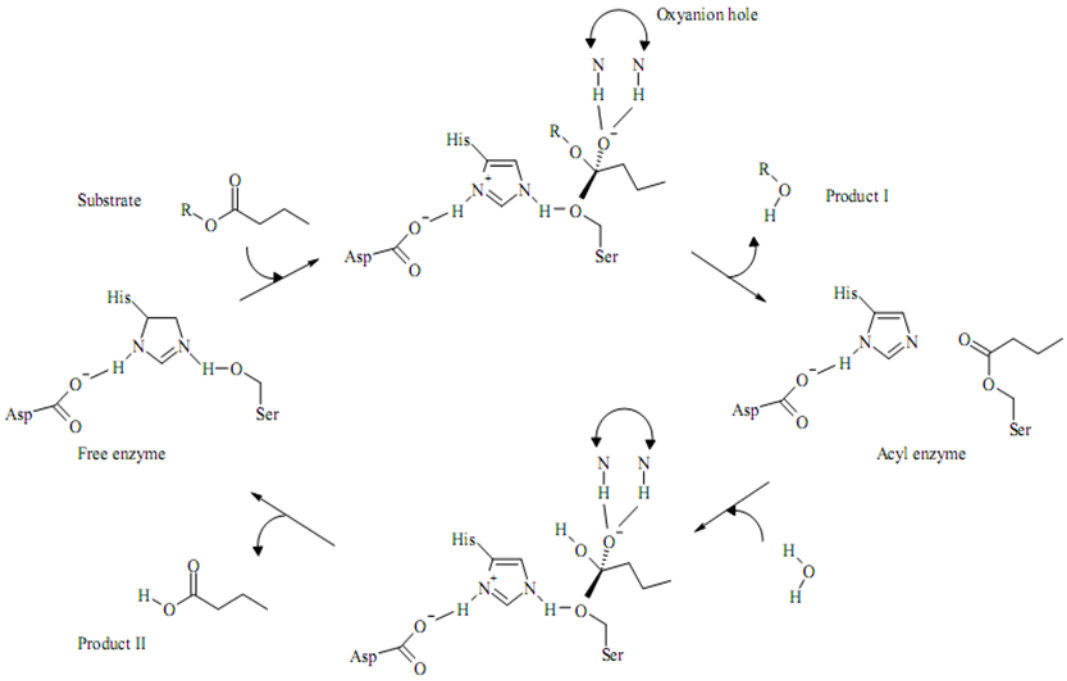



**Figure 1. 3.** Lipase Hydrolysis Mechanism of an Ester Bond (Holmquist, 2000).

## 1.2.2 Properties of *Pseudomonas* lipases

Studies on bacterial lipases have classified them into eight families based on amino acid sequence homology. Lipases from the genus *Pseudomonas* belong to the family I, which is the largest group, and have been classified into sub family I.1, I.2 and I.3. These are often referred to as the true lipases as they have contributed to the general understanding of lipase function and activity. Sub family I.1 and I.2 require a lipase-specific foldase (Lif), a chaperone-like protein, for their functional expression and secretion. Lipases such as the *Pseudomonas aeruginosa* and *Burkholderia glumae* (formerly known as *Pseudomonas*) exhibit such characteristics and have a molecular mass in the range of 30-33 kDa (Aripigny and Jaeger, 1999; Zhang *et al.*, 2009). Their secretion is mediated by a classic signal peptide through the cell membrane and is known as type II secretion. Sub family I.3 consists of two distinct lipases from *P. fluorescens* and *Serratia marcescens* with a higher molecular weight as compared to

subfamily I.1 and I.2, 50 kDa and 65 kDa respectively. These lipases have a C- terminal-targeting signal instead of a typical N-terminal signal peptide and use the type I secretion. The *Pseudomonas* lipases have specific properties, that is, optimal pH and temperature, stability in the presence of organic solvents and metal ions and substrate specificity that may vary based on which group the enzyme belongs to (Rios *et al.*, 2018).

#### 1.2.2.1 Effect of pH and Temperature

Enzymes are protein in nature, meaning they are composed of amino acids whose ionization can be affected by changes in pH. Bacterial lipases from *Pseudomonas* have been found to have a neutral or alkaline optimum pH which is mainly influenced by the primary and secondary structure of the lipases (Latip *et al*., 2016). Studies conducted on *P. fluorescens* SIK W1 found that it had an acidic optimum of pH 4.8. Other species such as the *Pseudomonas* sp. KWI-56 and *P. cepacia* DSM 50181 also had an acidic optimum of 5.0 and between 5.5-7, respectively. Bacterial lipases substantially possess a wide range of pH stability, that is, from pH 4 to pH 11 (Facchin *et al.*, 2013; Verma *et al.*, 2012).

Industrial processes operate at high temperatures that exceed 45 °C hence the need of thermophilic lipases that are stable and functional at high temperatures. Temperature optima of the *Pseudomonas* lipases has been found to range from 30-60 °C and have been widely used as biocatalysts in organic synthesis (Schmidt *et al*., 2010; Sharma *et al.*, 2002). Thermotolerant lipases have been reported such as the *P. fluorescens* Pf0-1 that was characterised and found to have an optimal temperature of 70 °C and remains active at high temperatures, between 80-100 °C. Addition of stabilisers such as glycol, has been reported to also increase thermostability of lipases (Nawani and Kaur, 2000; Liu *et al.*, 2017). Some of the *Pseudomonas* that have been studied are shown in Table 1.1 below.

**Table 1. 1:** Properties of *Pseudomonas* lipases in literature.

| Lipase | Weight (kDa) | pH opt. | pH stability | pI [a] | Optimum temp. (°C) | Reference |
|---|---|---|---|---|---|---|
| **Lipase from *P. aeruginosa* EF2** | 29 | 9.0 | 4.0-10.0 | 4.9 | 50 | Gilbert *et al*., 1991 |
| **Lipase from *P. Fragi* 22.39B** | 33 | 9.0 | 4.0-11.0 | 6.9-7.0 | 65-70 | Gupta *et al*., 2004 |
| **Lipase from *P. Fluorescens* AK 102** | 33 | 8.0-10.0 | 4.0-10.0 | 4.0 | 55 | Gilbert, 1993 |
| **Lipase from *P. Fluorescens* P26504 LipA*** | 48.2 | 8.4 | - | 8.6 | - | ProtParam. |
| **Lipase from *Pseudomonas sp*. (PSL)** | 30 | 7.0-9.0 | 6.0-12.0 | 4.5 | 45-60 | Gupta *et al*., 2004 |

a) Isoelectric point

*lipase expressed and purified in this study

### 1.2.2.2 Effect of metal ions and stability in organic solvents

Effect of metal ions has been studied to determine whether they enhance or reduce enzyme activity. Metal cations play an important role particularly in the structure and function of *Pseudomonas* lipases, which have been found to be calcium dependent. Divalent cations have been found to specifically enhance enzyme activity (Verma *et al.*, 2012). A study on *P. fluorescens* AMS8 showed that calcium ($Ca^{2+}$) played a structural role as compared to a catalytic role in other lipases. The $Ca^{2+}$ binds to the enzyme leading to a conformational change to the protein, increasing stability. A hypothesis was made that the better interfacial activation that occurred after addition of $Ca^{2+}$ might have been caused by the metal ion eliminating unfavourable electrostatic repulsions on the protein (Yaacob *et al.*, 2016). Another study conducted on *P. cepacia*, found that $Ca^{2+}$ played a catalytic role in the enzyme by causing conformational changes that expose the active site, hence providing a hydrophobic surface for interaction with the substrate. Other metal ions such as zinc ($Zn^{2+}$) and iron ($Fe^{2+}$) have been found to strongly inhibit *Pseudomonas* lipase activity (Schrag *et al.*, 1997; Sharma *et al*., 2001).

In general, enzymes are not stable in the presence of organic solvents as they are quick to denature. Organic solvents inactivate enzymes by exposing hydrophobic residues and removing crucial water molecules, thereby decreasing conformational flexibility. However, *Pseudomonas* lipases have been reported to be organic solvent-tolerant and non-polar solvents tend to facilitate the interfacial activation of lipases thereby increasing their activity. Activity tends to be lost when organic solvents are added at concentrations higher than 10-20 % (Gupta *et al.*, 1997; Rios *et al*., 2018). In addition to interfacial activation, non-polar solvents enhance the solubility of the substrate in the reaction. *Pseudomonas* lipases have been shown to exhibit

increased activity, stability and enantioselectivity in non-polar organic media. Different *Pseudomonas* lipases show distinct stabilities against various organic solvents with studies conducted on *P. aeruginosa*, *Pseudomonas* sp., *Burkholderia cepacia*, and *P. fluorescens* 5693 to mention a few (Peng *et al*., 2009; Zhang *et al*., 2009).

### 1.2.2.3 Effect of Chelating Agents and Surfactants

Studies on the stability of *Pseudomonas* lipases with chelating agents and surfactants has been shown to be linked to the presence of calcium ($Ca^{2+}$) ions on the enzyme. Surfactants increase the water-lipid interface hence increasing enzymatic activity of *Pseudomonas* lipases. However, some surfactants have been found to affect the enzyme depending on their concentration. A study on *P. aeruginosa* and *P. fragi* showed that they experienced inhibition in the presence of cationic and anionic surfactants. SDS, an anionic surfactant, was inhibitory at 0.05 mg/ml. It was discovered that it bound to the $Ca^{2+}$ ions and caused unfolding of the proteins. The *P. fluorescens* enzyme was stable in both anionic and cationic surfactants. EDTA, a chelating agent, has been known to affect metallolipases. A study on the lipase *BK* – AB18 showed a decrease in activity of 40 % after adding EDTA and a decrease of 50 % in the presence of $Ca^{2+}$ ions. Lipases such as the *P. aeruginosa* and *P. fluorescens* were also inhibited by EDTA. Lipases with loosely bound $Ca^{2+}$ ions are likely to be affected by surfactants and chelating agents (Hertadi *et al*., 2015; Svendsen *et al*., 1995).

Another denaturing agent, PMSF, was investigated on how it affects the activity of the *P. cepacia* lipase. PMSF is a serine protease inhibitor. The active site of lipases contains a serine residue that is one of the key amino acids for catalysis to occur. PMSF (15 mM) inhibited the activity of the *P. cepacia* by 34.7 % (Kanwar *et al*., 2015).

### 1.2.2.4 Substrate specificity

Substrate specificity of lipases has led to their intensive research and use in the organic synthetic industry. They exhibit properties like regio-, chemo- and stereo-specificity. International nomenclature states that lipases hydrolyse triacylglycerols and based on regioselectivity, they have been classified into three categories according to structures and

position of the fatty acids (Javed *et al*., 2018). Proposed classification of lipolytic enzymes is divided into 1) non-specific lipases liberating fatty acids from any position (mono-, di-, tri-); 2) positional specificity hydrolysing only primary ester bonds at C1 and C3 of glycerol (referred to as 1,3 specific) and lastly 3) lipases that have a fatty acid preference and liberate fatty acids from any position as long as it is unsaturated (Davranov and Khalameizer, 1997; Jaeger *et al*., 1994).

Taking into consideration that lipases also hydrolyse other esters, enantioselectivity (stereo-specificity) has been demonstrated on racemic mixtures of secondary alcohols. Enzyme selectivity depends on either hydrophobicity or the size of the molecules at the stereo-centre of the secondary alcohol (Kazlauskas *et al*., 1991). In general, no quantitative correlation between secondary alcohol structure and enantioselectivity has been established with studies conducted on *P. cepacia* showing high enantioselectivity (*E*) for *M* (medium sized molecules) = $CH_3$ and *L* (large molecules) = $C_6H_5$, but low for more-bulky *L* = $C_4H_4$-*p*($OCH_3$), Figure 1.4. *E* was found to be medium for *L* = $CH{=}CHC_6H_5$ and *M* = $CO_2H$ and high for a larger *M* = $CO_2CH_2CH_3$ (Schulz *et al*., 2000).

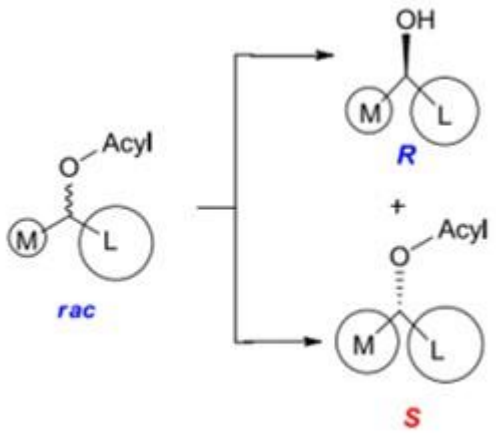



**Figure 1. 4:** Secondary alcohol consisting of two substituents of different sizes. L represents the large substituent and M a medium-sized substituent.

Interaction between substrate and lipase also plays an important part in stereoselectivity. Solvents also play an important role since the substrate is dissolved in these solvents creating the water-lipid interface. During interfacial activation, the catalytic triad (active site) and non-polar residues on the lid are entirely exposed, interacting with the hydrophobic medium

forming what is referred to as the binding pocket. The carbonyl group of the substrate is enabled to bind to the catalytic triad with its acyl chain binding to the non-polar hydrophobic area created by the lid and enzyme. Acyl chain length, degree of unsaturation and the location of double bonds on the chains have been postulated to influence selectivity (Muralidhar *et al*., 2002). The binding pocket size and geometry has also been related to enantioselectivity as docking studies showed that two enantiomers bind in different orientations, enabling one of the two to react faster than the other (Santarossa *et al.*, 2005).

*Para*-nitrophenyl esters have been particularly used to determine hydrolytic activity of lipases. Selectivity based on chain length and unsaturation is demonstrated using *p*-nitrophenyl esters (Pencreac'h and Baratti, 1996). Various *Pseudomonas* lipases have been shown to prefer different chain lengths of these *p*-nitrophenyl esters, $C_2$ – $C_{16}$, hence each lipase must be investigated separately from the other. A study on *Pseudomonas fluorescens* JCM 5963 showed high activity towards *p*$NPC_8$ (*p*-nitrophenyl caprylate) and moderate activity towards shorter chained esters. Another study based on *Burkholderia cepacia* ATCC 25416 showed high activity towards *p*$NPC_{12}$ (*p*-nitrophenyl laurate) and very low activity towards short chain esters (Wang *et al*., 2009; Zhang *et al*., 2009).

### 1.2.3 Expression and Purification of *Pseudomonas* Lipases

Expression of *Pseudomonas* genes has been relatively straight forward in prokaryotic systems such as *E. coli*, that have been found to be efficient sources of recombinant protein production. Various *E. coli* strains are able to obtain high cell density and in-turn a higher concentration of the desired product (Studier *et al*., 2009). The *E. coli* strain BL21 (DE3) strain and its derivatives have been widely used in overexpression of recombinant proteins. It contains a λDE3 lysogeny that harbours the gene for the bacteriophage T7 RNA polymerase, which drives recombinant protein production in *E. coli* cells. It is only selective to its own promoters that are absent in natural *E. coli* cells. The T7 is dependent on the *lac*UV5 promoter, which is controlled by a *lac* repressor *lac*I, and is very sensitive to catabolite repression. In the presence of an inducer, IPTG, the *lac*I is relieved allowing recombinant protein production (Shiloach *et al*., 1996; Wagner *et al*., 2008). A major disadvantage of using these *E. coli* systems is that they lack posttranslational modifications, hence insufficient folding of complex proteins from

higher organisms. These recombinant proteins tend to express as insoluble and inactive proteins (Winkler *et al*., 2012).

*Pseudomonas* lipases from the subfamily I.1 and I.2, including *P. aeruginosa* and *B. cepacia*, have been found to express in a similar manner with the aid of a lipase-specific foldase (Wang *et al*., 2009). A study conducted on *P. aeruginosa* showed that the lipase was expressed in the bacterial cytoplasm of *E. coli* cells as enzymatically inactive inclusion bodies. A controllable expression system was designed that consisted of the *P. aeruginosa* operon LipA/H that contained the signal sequence lipase fusion (Liebeton *et al*., 2001). The system also had a second copy of LipH (coding for the foldase protein) that had been cloned behind the T7 gene 10 promoter. This enabled the co-expression of the lipase and the foldase and in turn an enzymatically active lipase in a system known as *in vivo* folding (Akbari *et al*., 2010; Wu *et al.*, 2012). Another case of producing enzymatically active lipases from subfamily I.1 and I.2 was to express and purify the lipase and foldase separately; and then folding the lipase by mixing the two in a system known as *in vitro* folding (Alnoch *et al*., 2018).

To date, there have been a limited number of *Pseudomonas* species, for example *P. fragi* IFO 34584 and *P. fluorescens* C9, that have been expressed in *E. coli* cells in an enzymatically active form. A study conducted on *P. fluorescens* JCM5963 showed that the lipase expressed without the help of the foldase. However, the expression level was low and was achieved at a low temperature of 20 °C with an IPTG concentration of 0.05 mM (Zhang *et al*., 2009).

Enzyme purification has been done not only to isolate the lipase enzymes from contaminants but also to assist in improving their activity, stability and shelf life. Purification also enables the determination of the enzyme's structural elucidation, that is, primary amino acid sequences and three-dimensional structures in relation to their functions (Davidson, 1996). The initial steps of purification involve the concentration of the enzyme by extraction with organic solvents, ultra-filtration and ammonium sulfate precipitation. A combination of chromatographic steps, ion exchange, then follows depending on the desired level of purification (Javed *et al*., 2018). The most frequently used methods of ion exchange chromatography on lipase purification are anion exchange, which involves the use of ion exchangers such as the diethylaminoethyl (DEAE) group, and the cation exchangers based on the carboxymethyl (CM) group. Lipase purification is sometimes troublesome, time consuming and may result in low lipase yields (Saxena *et al*., 2003).

## 1.2.4 Industrial Uses of Lipases

*Pseudomonas* lipases are a versatile tool in biocatalysis due to their ability to catalyse a variety of reactions such as esterification, interesterification, acidolysis, alcoholysis and aminolysis in addition to their desirable hydrolytic action. They produce enantiomerically pure compounds hence the growth of their uses in industrial synthetic chemistry, as summarised in Figure 1.5 (Houde *et al.*, 2004). *Pseudomonas* lipases have been active in industry because most of the synthetic reactions conducted in industrial scale are carried out in organic solvents which enable solubility of non-polar compounds (Kumar *et al.*, 2016). They also have been found to be stable at high temperatures convenient for industrial processes, that is, between 30-60 °C. However, when these lipases are immobilised, they can be used at temperatures as high as 70 °C for prolonged periods (Andualema and Gessesse, 2012).

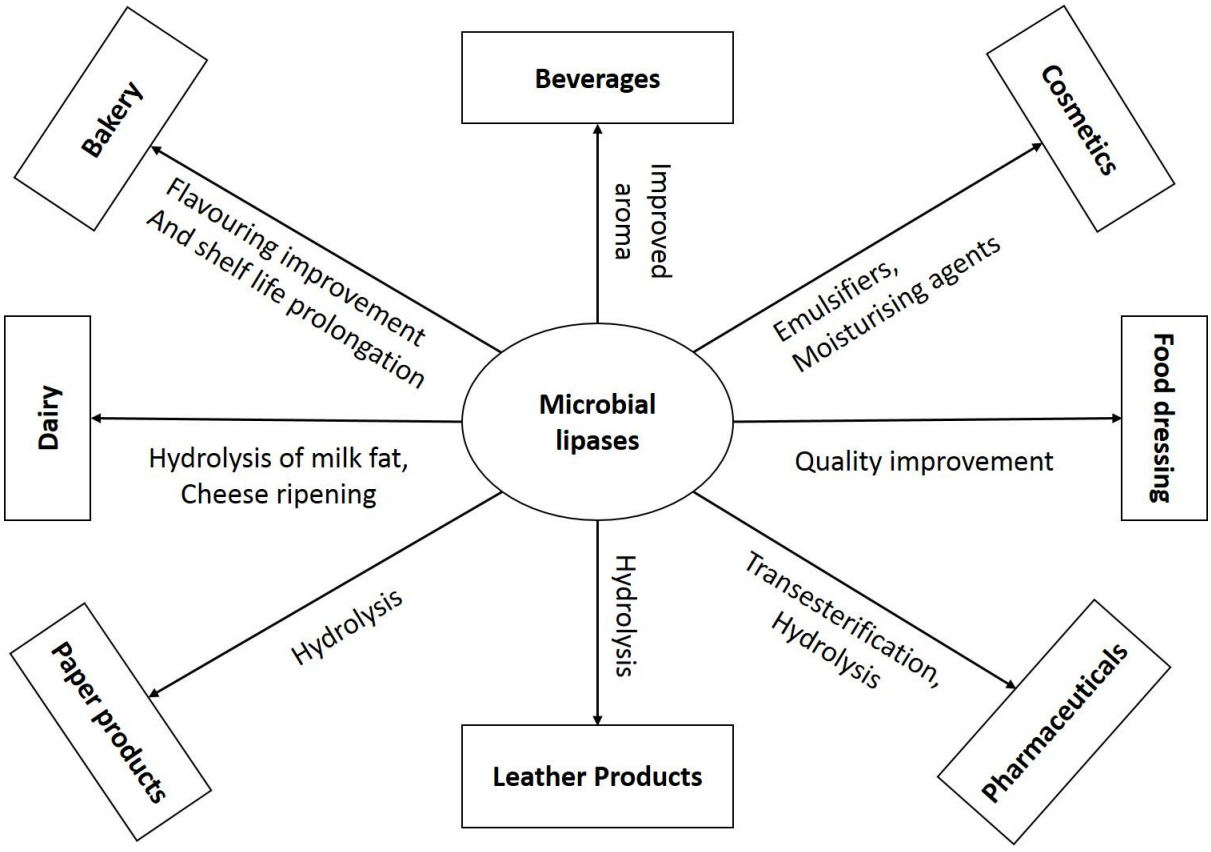



**Figure 1. 5**: Various Industrial Applications of Lipases (Angajala *et al*., 2016)

### 1.2.4.1 Lipases in the Food Industry

The ability of lipases to hydrolyse fatty acids has been one of their special characteristics exploited in the food industry. Fats and oils are essential constituents in foods which at times can be desirable, particularly in the meat industry (Verma *et al*., 2012). Lipases are used to remove fat from meats and fish in a process called bio-lypolysis. Lipases are also applied in flavour development of foods by synthesising short chain fatty acids and alcohols that are referred to as flavour compounds. They have been applied in cheese ripening, butter, margarine and alcoholic beverage development. Enzymes such as the *Pseudomonas* strain P38 and some *Pseudomonas* sp. have been widely used (Tan *et al*., 1996).

### 1.2.4.2 Lipases in the Detergent Industry

Hydrolytic lipases have been widely applied in the detergent industry with more than half of all the detergents containing these enzymes. Household and laundry detergents used in dishwashers and washing machines usually contain two or more enzymes to improve efficiency. Lipases have been used mainly because they meet the criteria required for detergent enzymes (Jaeger and Reetz, 1998). Lipases have a low substrate specificity hence they hydrolyse a wide range of fats and can withstand surfactants which also make up the composition of detergents and can also withstand harsh conditions (pH 10 - 11; 30 - 60 °C) that the dishwashers and washing machines operate at. *Pseudomonas mendocina* and *P. alcaligenes* play an important role in cleaning detergents as they can hydrolyse organic waste in toilet bowls and sinks (Kazlakaus and Bornscheur, 1998).

### 1.2.4.3 Lipases in Biofuels

The ability of lipases to conduct transesterification has been exploited in biodiesel production. Green chemistry approaches in industrial synthesis have led to the use of biocatalysts in biodiesel production with the aim of reducing toxic wastes. Biodiesel is defined as long chain alkyl (methyl, ethyl or propyl) esters of vegetable oil or animal fat-based diesel fuel. It is

synthesized by a transesterification reaction between a lipid and a short chain alcohol. The most common lipase that has been used in biodiesel production but has not yet been commercialised, is the *P. cepacia* (Andualema and Gessesse, 2012; Sangeetha *et al*., 2011).

#### 1.2.4.4 Lipases in Organic Synthesis

The high demand for regioselective and stereoselective transformations in organic synthesis has led to the use of enzymes. Lipases have demonstrated adaptability to industrial organic synthesis conditions and initiate various reactions as mentioned earlier. *Pseudomonas* lipases have been widely used in the production of chiral chemicals. These serve as basic building blocks in the synthesis of pharmaceuticals, insecticides and pesticides (Andualema and Gessesse, 2012). A good example of the use of the *Pseudomonas* lipases is in the production of enantiopure Morita-Baylis-Hillman adducts.

## 1.3 Morita-Baylis-Hillman Reaction

The Morita-Baylis-Hillman (MBH) reaction is one of the most important carbon-carbon bond forming reaction in organic synthesis. The reaction occurs between an electrophilic aldehyde and the α position of an activated alkene connected to an electron-withdrawing group. Aldehydes react with alkenes such as acrylonitrile, methyl vinyl ketone and ethyl or methyl acrylate, to form α-methylene-β-hydroxy compounds (Figure 1.6). This reaction is catalysed by a tertiary amine or phosphine which acts as a nucleophilic catalyst. The most common amine used is 1,4-diazabicyclo [2.2.2] octane (DABCO) (Xavier *et al.*, 2014; Yadav *et al*., 2007).

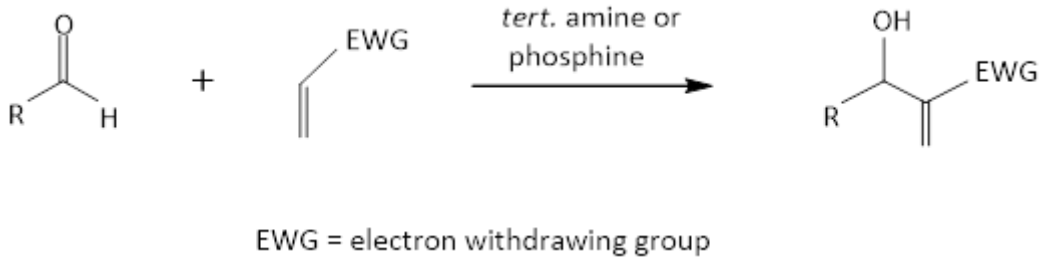
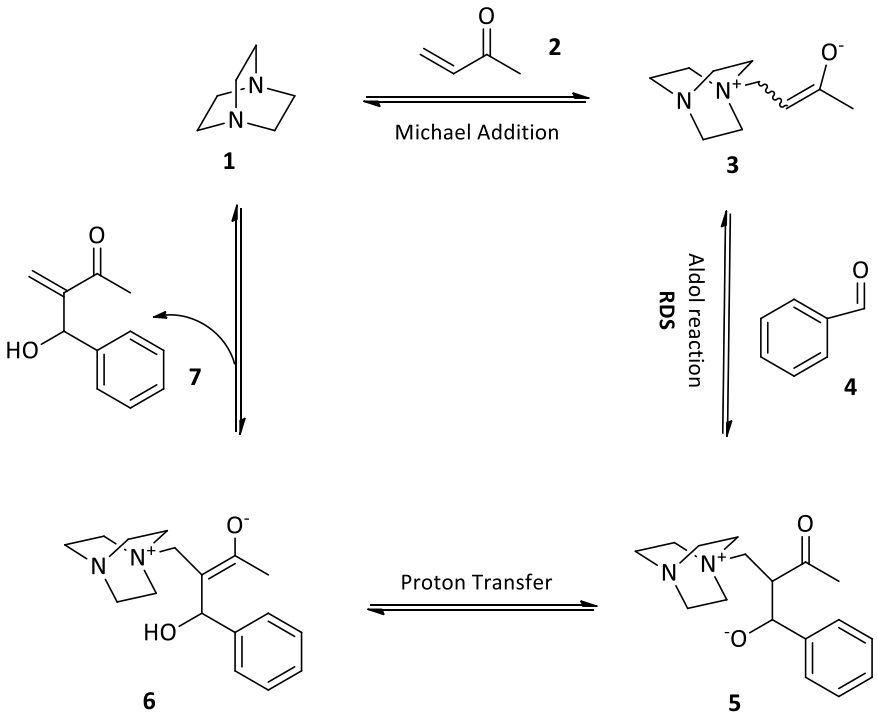



**Figure 1. 6**: Morita-Baylis-Hillman reaction (Juma *et al*., 2017)

The mechanism of the reaction proceeds in three steps and catalysis starts with the Michael addition of the nucleophilic trigger, DABCO (**1**), to the activated alkene (**2**, Figure 1.7). A zwitterionic adduct **3** is generated and it undergoes an aldol reaction with the aldehyde **4** to form **5**. Subsequent intramolecular proton transfer protonates the alcohol and forms an enolate **6**. In the last step, the product (**7**) is released, together with regenerated catalyst (**1**) in an elimination reaction (Langer, 2000).




**Scheme 1. 1**: Generally accepted MBH reaction mechanism

The MBH reaction plays a significant role in synthetic chemistry and medicinal chemistry and it also conforms to the development of green chemistry standards. It has intrinsic credentials such as solvent free conditions, high atom economy, organo-catalysis, eco-friendly and wide functional group tolerance (Reddy and Rao, 2018). Morita-Baylis-Hillman adducts (MBHAs), also known as α-methylene-β-hydroxy compounds, and their acetate, carbonate or bromide derivatives are suitably functionalised for a multitude of chemical transformations (Figure 1.8). They exhibit several bioactivities, for example, antibacterial, antifungal and anti-malarial (Zhang *et al.*, 2007).

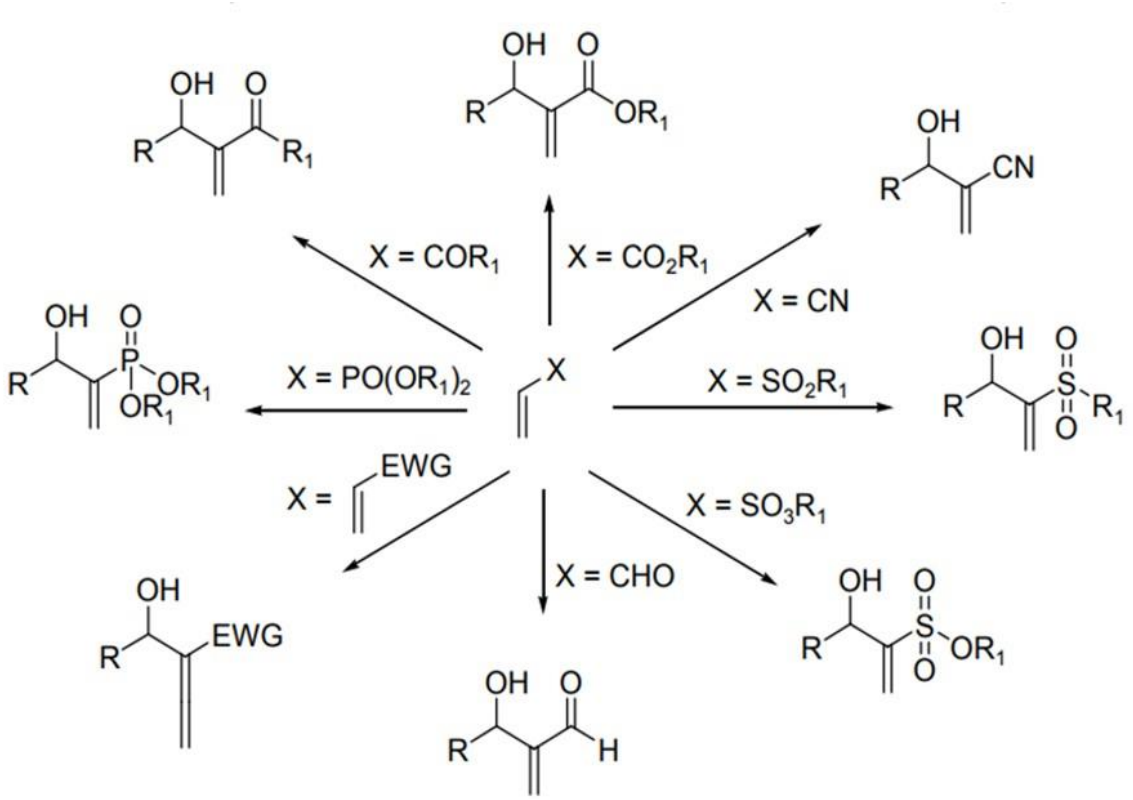



**Figure 1. 7**: MBH reaction with a wide variety of activated alkenes. Reaction is conducted with aldehydes at atmospheric pressure and DABCO catalyst.

MBH adducts (MBHAs) are synthesised in racemic form, in the absence of chiral auxiliaries, and convenient routes to asymmetric reactions have not been exploited due to their low reactivity (Nascimento *et al.*, 2003). Hydrogenation of the racemic products in the presence of a mono-chiral transition-metal catalyst has been one of the procedures done to obtain enantiopure MBHAs, however, limitations became evident due to some molecules having other functional groups that are vulnerable to reduction. Enzymatic kinetic resolution is highly used with lipases performing both transesterification of the hydroxyl forms and hydrolysis of the acetate derivatives (Burgess and Jennings, 1990; Hayashi *et al.*, 1998).

## 1.3.1 Lipase-Catalysed Kinetic Resolutions of MBHAs

A kinetic resolution is a key tool that can be employed in the synthesis of optically pure MBH adducts. The kinetic resolution is a process whereby one of the enantiomers is transformed to the corresponding product faster than the other. The enantiomer being transformed achieves a

maximum theoretical yield of 50 %, thus there is only 50 % conversion with the other enantiomer remaining unchanged (Li *et al*., 2016). Previous studies have shown that lipases from *Pseudomonas* sp. have been used in the optimisation of kinetic resolutions of MBH adducts and transesterification reactions. *Pseudomonas* sp. lipases have been used in the kinetic resolution of ferrocene derivatives. These chiral ferrocene derivatives are ideal starting materials in the synthesis of terpenoids and carotenoids (Alba and Rios, 2009; Nascimento *et al*., 2003).

Racemic α-methylene-β-hydroxy esters have also been resolved using lipases. A *Pseudomonas* AK lipase and a *Pseudomonas* sp. showed good enantioselectivity towards the ester and moderate results towards the alcohol derivative. Low enantiomeric values were observed for the alcohol derivatives containing R = $CH_3$ groups or large side chains R > $C_2H_5$. Another MBH adduct that has been studied is (±) -2-[hydroxy(*m*-nitrophenyl)methyl]acrylonitrile and its *ortho* nitro isomers. A kinetic resolution was conducted on this MBH adduct using four different lipases, that is, *Candida antarctica* lipase B, *Pseudomonas cepacia*, *Candida rugosa* and *Aspergillus niger*. Highest enantioselectivity was exhibited by the *C. antarctica* and moderate activity by the *P. cepacia*. Structure of the MBH adducts also proved to be a factor in the kinetic resolutions. The kinetic resolution did not take place when the nitro group was positioned in the *ortho* position of the aromatic ring. This corresponded to the studies based on the enzymatic interactions with the substrates (Kazlauskas *et al*., 1991; Xavier *et al*., 2014).

## 1.4 RATIONALE

Morita-Baylis-Hillman adducts (MBHAs) are synthesized in racemic forms and their separation has been a challenge over the years. The growing demand and wide application of enantiopure compounds has led to the use of enzymes to obtain enantiopure MBHAs. Previous lipase-resolution studies on MBHAs have generally been found to be successful, with the best overall resolution from a *Pseudomonas fluorescens* lipase. However, the *Pseudomonas fluorescens* lipase (product 95608 from Sigma-Aldrich®) is no longer produced commercially hence the need to express and purify the enzyme to conduct kinetic resolution reactions on MBHAs.

# 2 AIM AND OBJECTIVES

## 2.1 Aim

The aim of this research was to express and partially purify the *Pseudomonas fluorescens* lipase (P26504 LipA_Psefl) and conduct a kinetic resolution on Morita-Baylis-Hillman acetates to obtain enantiopure Morita-Baylis-Hillman adducts.

## 2.2 Objectives

- Transform pET11a plasmid harbouring the *P. fluorescens* P26504 LipA_Psefl gene into *E. coli* JM109 and BL21 (DE3) pLySs cells
- Heterologous overexpression and partial purification the *P. fluorescens* lipase
- Conduct the Morita-Baylis-Hillman reaction to form Morita-Baylis-Hillman adducts and corresponding acetates
- Conduct the kinetic resolution on the MBH acetates to obtain enantiopure MBHAs using the *P. fluorescens* lipase

# 3 METHODS AND MATERIALS

## 3.1 Preparation of competent cells

*Escherichia coli* JM109 strain was grown in 2YT agar (16 g Tryptone, 10 g Yeast Extract, 5 g Sodium Chloride, 15 g Agar) at a temperature of 37 °C overnight. A single colony was inoculated into 5 ml 2YT broth in 50 ml falcon tube and grown overnight at 37 °C. An aliquot (1 ml) overnight culture was sub-cultured into 100 ml fresh 2YT-amp$^{+}$ (ampicillin 100 mg/ml stock: 1 g sodium ampicillin in 10 ml $dH_2O$) broth in a 250 ml volumetric flask and grown to early log phase 0.4-0.6 at $OD_{600}$ for 2-4 hours. Cells were cooled in ice for 10 minutes and collected by centrifugation at 3000 x g at 4 °C for 10 minutes. Cells were re-suspended in 10 ml of 0.1 M magnesium chloride ($MgCl_2$) and incubated in ice for 30 minutes and then centrifuged at 3000 x g at 4°C for 10 minutes. Supernatant was discarded, and pellet re-suspended in 5 ml cold 0.1 M CaCl/15 % Glycerol solution. Aliquots (50 µl) were dispensed in microtubes and stored at -80 °C. Same procedure was done for *E. coli* BL21 (DE3) pLysS strain with the addition of a working solution of 35 µg/ml chloramphenicol (chloramphenicol 35 mg/ml stock: 350 mg chloramphenicol in 10 ml 95% ethanol) in the 2YT agar and broth.

## 3.2 Transformation

An aliquot (1 µl) of pET11a plasmid from GenScript containing the *Pseudomonas fluorescens* lipase gene was added into a microtube containing JM109 competent cells. A control tube containing JM109 competent cells with 1 µl $dH_2O$ was set up. Cells were incubated in ice for 30 minutes. Samples were heat shocked by placing them in a 42 °C heating block for 45 seconds then removed and incubated in ice for 5 minutes. Super optimal broth with catabolite repression (SOC: 2 % w/v Tryptone, 0.5 % w/v Yeast Extract, 10 mM NaCl, 2.5 mM KCl, 10 mM $MgCl_2$, 10 mM $MgSO_4$, 20 mM Glucose), 200 µl, was added and cells incubated at 37 °C for 2 hours whilst shaking. An aliquot, 200 µl and 20 µl, was plated and spread on 2YT-ampicillin (100 µg/ml) agar plates and incubated overnight at 37 °C. A colony containing pET11a plasmid was picked, inoculated into 50 ml 2YT-ampicillin broth and incubated at 37 °C overnight. Aliquot (500 µl) were added into snap-top tubes containing 500 µl of 50 % glycerol solution and stored at -80 °C.

## 3.3 Plasmid Extraction and Confirmation

Plasmid extraction was done using the Zyppy™ Plasmid Miniprep Kit. The buffer was prepared by adding 24 ml (26 ml) 100 % (95 %) ethanol to 6 ml Zyppy™ wash buffer concentrate. An aliquot (1.5 ml), from the 50 ml 2YT-ampicillin broth and incubated at 37 °C overnight, was added into a 2 ml microcentrifuge tube and centrifuged at 14,000 x g on the Eppendorf Mini Spin Plus centrifuge. Supernatant was discarded and 600 µl of TE (10 mM Tris- 1 mM EDTA, pH 8) buffer was added to the pelleted cells and resuspended completely. Into the microcentrifuge tube containing suspended cells, 100 µl of 7X Lysis buffer (blue) was added and mixed by inverting 5 times. The mixture was incubated at room temperature for 2 minutes. An aliquot (350 µl) of cold neutralisation buffer was added and mixed thoroughly and centrifuged at 11,000 x g for 4 minutes. Supernatant was transferred into a Zymo-Spin™ IIN column, placed into a collection tube, and centrifuged for 15 seconds at 11,000 x g. Flow through was discarded and Zymo-Spin™ IIN column returned to the same collection tube. Endo-Wash buffer, (200 µl), was added to the column and centrifuged for 30 seconds at 11,000 x g. Zyppy™ Wash Buffer, (400 µl), was added to the column and centrifuged at 11,000 x g for 1 minute. The column was then transferred into a clean 1.5 ml microcentrifuge tube and an aliquot (30 µl) of Zyppy™ Elution buffer added directly to the column matrix. The column was incubated at room temperature for 1 minute and centrifuged at 11,000 x g for 30 seconds to elute the plasmid DNA. Concentration was determined using the Invitrogen Qubit® 2.0 Fluorometer.

### 3.3.1 Restriction Digest

The restriction enzymes, ultra-pure water and buffers used for restriction digest were all purchased at Thermo Fisher Scientific. Four 0.2 ml PCR tubes were labelled 1 to 4. An aliquot 2 µl of red buffer was added into all the tubes. Into tube one, 13 µl of ultra-pure water and 5 µl of sample were added. Into tube two, 11 µl of ultra-pure water, 2 µl of BamHI and 5 µl of sample were added. Into tube three, 11 µl of ultra-pure water, 2 µl of NdeI and 5 µl of sample were added. Into tube four, 9 µl of ultra-pure water, 2 µl of BamHI, 2 µl of NdeI and 5 µl of sample were added. All the reaction tubes contained 20 µl in total. Tubes were incubated in the PCR machine at 37 °C for 1 hour and inactivated at 65 °C for 20 minutes. Restriction products

were prepared for gel electrophoresis by adding 5 µl of sample to a PCR tube containing 2 µl of 6X Mass-Ruler DNA loading dye and run on an agarose gel for confirmation.

### 3.3.2 Agarose Gel Electrophoresis Confirmation

CSL-AG 100 LE Multi-Purpose Agarose from Cleaver Scientific Ltd was used. One-gram agarose powder was weighed and dissolved in 100 ml 1X TAE buffer (50X TAE: 242 g Tris base, 18.61 g Disodium EDTA, 57.1 ml Glacial Acetic Acid, dH2O to 1 litre) by gradually heating in a microwave. Liquid was left for 5 minutes to cool to 50 °C and 2 µl ethidium bromide was added. Bio-Rad casting tray aligned with the comb were set and the gel was poured and left at room temperature for 30 minutes to set. An aliquot 3 µl of Gene-Ruler 1 kb DNA ladder was loaded on the gel wells together with 5 µl restriction samples and run at 90 V for 45 minutes. The gel was viewed on the Bio-Rad gel doc.

## 3.4 Expression Trials

Expression trials were conducted in order to identify the desirable conditions for expression of *Escherichia coli* BL21(DE3) pLysS containing the pET11a plasmid. The effect of temperature, Isopropyl-β-D-thiogalactopyranoside (IPTG) concentration and induction periods were tested. Transformed cells were inoculated in 50ml 2YT broth containing 35 µg/ml chloramphenicol and 100 µg/ml ampicillin and grown, shaking, overnight at 37 °C. The culture was inoculated into 500 ml Erlenmeyer flasks containing 100 ml of the same medium (2YT-$Amp^+$-$Chloram^+$), labelled 0, 0.3, 0.6, 1.0 (representing IPTG concentration), at a dilution factor of 1:20. Flasks were incubated at 37 °C for 2 hours to early log phase of 0.4-0.6 at $OD_{600}$. Isopropyl-β-D-thiogalactopyranoside (IPTG stock: 2.38 g IPTG in 10 ml $dH_2O$) was added at different concentrations (0.3 mM, 0.6 mM, 1.0 mM) corresponding to the labels and incubated at 37 °C for 24 hours. An aliquot (2 ml) of bacterial cultures grown in 2YT-$Amp^+$-$Chloram^+$ were collected at 4-, 8-, 12- and 24 hours, and pelleted using an Eppendorf Mini Spin Plus centrifuge at 11,000 x g for 2 minutes.

The cells were re-suspended in 500 µl of 20 mM Tris-HCl buffer, pH 8.00 (standard buffer, unless otherwise stated), containing 1 mM phenylmethylsulfonyl fluoride (PMSF). Thereafter,

the samples were frozen at -20 ℃. The cells were thawed at room temperature and lysed by sonication using a QSonica sonicator. The lysed cells were centrifuged for 10 minutes at 11,000 x g using the Eppendorf Mini Spin Plus centrifuge. The supernatant was mixed with reducing SDS-PAGE sample buffer (10 ml 4X stock: 1 M Tris-HCl pH 6.8, 1 g SDS, 0.5 ml dH2O, 0.8 ml 0.1% Bromophenol blue, 4 ml 100 % glycerol, 2 ml 14.3 M β-mercaptoethanol) at a ratio of 1:3. The pellet was re-suspended in 500 µl of 20 mM Tris-HCl buffer, pH 8.00, containing 1 mM PMSF and mixed with reducing sample buffer and electrophoresed as per the protocol described by Schagger, (2015). Ten microlitres of the expression trials samples containing reducing sample buffer were electrophoresed using 16 % polyacrylamide gels. The procedure was repeated at 20-, 25- and 30 °C to investigate effect of temperature.

## 3.4.1 Sodium Dodecyl Sulfate-Polyacrylamide Gel Electrophoresis (SDS-PAGE)

### 3.4.1.1 Solution Preparation

Separation gels with different concentration of monomers (acrylamide and bisacrylamide) and percentage concentration of the crosslinker relative to the total concentration, which were afterwards indicated with T and C, respectively, were prepared. The acrylamide-bisacrylamide (AB)-3 stock solution (T = 49.5%, C = 3% mixture) was prepared by dissolving acrylamide (48 g) and bisacrylamide (1.5 g) in $dH_2O$ (40 ml) and then adding $dH_2O$ up to 100 ml. Staining solution was prepared by mixing acetic acid (100 ml), Coomassie dye (0.25g) and $dH_2O$ (900 ml). De-staining solution was 10% acetic acid solution(v/v). Glycerol was prepared by diluting glycerol (80 ml) in $dH_2O$ (20ml). Ten percent SDS solution (w/v) was obtained by dissolving SDS (0.1 g) in $dH_2O$ (100 ml). Ten percent ammonium persulphate (APS) solution (w/v) was prepared by dissolving ammonium persulphate (0.1 g) in $dH_2O$ (1 ml). Electrode solutions were prepared by weighing the buffer contents as indicated in Table 3.1 below. The pH values of the buffers were adjusted by adding concentrated hydrochloric acid after adding 800 ml $dH_2O$ and 80 ml $dH_2O$ in the Gel buffer. Buffer solutions were made up to 1000 ml for the anode and cathode, and 100 ml for the gel buffer. The electrode buffers were diluted in a 1:10 ratio to $dH_2O$ for electrophoresis.

**Table 3. 1:** Electrode and gel stock solutions for SDS-PAGE

| | | Anode buffer (10×) [b] | Cathode buffer (10×) | Gel buffer [c] (3×) |
|---|---|---|---|---|
| Tris | (g) | 121 | 121 | 36.3 |
| Tricine | (g) | - | 179 | - |
| SDS | (g) | - | 10 | 0.3 |
| pH [a] | | 8.9 | 8.25 | 8.45 |
| $dH_2O$ to a Final Volume | (ml) | 1000 | 1000 | 100 |

a) pH was adjusted using concentrated hydrochloric acid
b) buffer concentration/strength
c) the gel buffer (3×) was filtered after adjusting pH

### 3.4.1.2 Gel Casting and Electrophoresis

The separating gel (16 %) was cast by adding AB-3 (10 ml), gel buffer 3× (10 ml), glycerol (3 ml) and $dH_2O$ (17 ml) into a falcon tube (50 ml). Ten percent APS (100 µl) and TEMED (10 µl) were added to the mixture and the gels immediately poured to the casting trays. An aliquot (300 µl) of $dH_2O$ were overlaid on the poured gels and left for 30 minutes to polymerise. The polymerised gels were overlaid with the 4 % stacking gel (AB-3 (1 ml), gel buffer 3× (3 ml), $dH_2O$ (12 ml), polymerised by adding APS (90 µl) and TEMED (9 µl)). The protein samples were mixed with the SDS-containing sample buffers and heated at 95 °C on the heating block. Gels were mounted in vertical BIO-RAD electrophoresis equipment. The cathode buffer as the inner electrode buffer and anode buffer as the lateral electrode buffer. The protein samples were loaded under the cathode buffer into the gel wells. Running conditions were set at 60 V initially and maintained at this voltage until the samples completely entered the lower separating gel. The next voltage steps were set at 100 V. The gel was viewed on the Bio-Rad gel doc.

### 3.4.1.3 Gel Staining

The gels were removed from the electrophoresis apparatus and then emerged fixing solution for 30 minutes. They were then stained in the staining solution for 1 hour. An absolute

background de-staining of the gels was performed by shaking the gels in 10% acetic acid for 2 hours with fresh de-staining solution and several times repeated.

## 3.5 Over-expression and Purification

Over-expression was conducted based on the best expression conditions found during the expression trials. An overnight culture (50 ml 2YT-amp$^{+}$-chloram$^{+}$), inoculated with *E. coli* BL21(DE3) pLysS containing pET11a plasmid, was grown at 37 °C for 24 hours. One litre 2YT broth was prepared and added into 5 litre flasks and autoclaved. The overnight culture was inoculated into the 5 litre flasks containing 1 litre of 2YT. An aliquot (500 µl) of antifoam was added to the media together with ampicillin (1 ml) and chloramphenicol (1 ml). Flasks were incubated at 37 °C for 2-4 hrs to early log phase of 0.4-0.6 at $OD_{600}$. After reaching OD, 1 ml IPTG (1mM) was added for induction. The flasks were incubated at 25 °C for 16 hours. Cells were harvested by centrifuging at 5,000 x g for 15 minutes in the Thermo Scientific™ Sorvall™ RC 6+ centrifuge. The cells were resuspended in 20 ml of 20 mM Tris-HCl buffer, pH 8.00, and disrupted by sonication at 20 second intervals for 1 minute. Thereafter, the sample was centrifuged at 25,000 x g for 30 minutes in the Thermo Scientific™ Sorvall™ RC 6+ centrifuge. The supernatant was transferred into a new set of falcon tubes (50 ml) and re-centrifuged in the same conditions.

Purification was done on the Äkta Prime Plus. A HiTrap DEAE Sepharose FF column (GE Health Care®) (5 ml) was mounted on the Äkta Prime Plus and equilibrated with 20 mM Tris-HCl buffer, pH 8.00. The protein was loaded on to the column and flow-through collected. Thereafter, the protein was eluted at a (50 ml) linear gradient of 0-1 M sodium chloride (NaCl) with standard buffer and ten, 5 ml, fractions were collected. The fractions were then applied to preparative SDS-PAGE. The protein eluted was desalted and concentrated by dialysis on Thermo Scientific SnakeSkin® Dialysis Tubing (10,000 MWCO) against the standard buffer and kept at -20 °C.

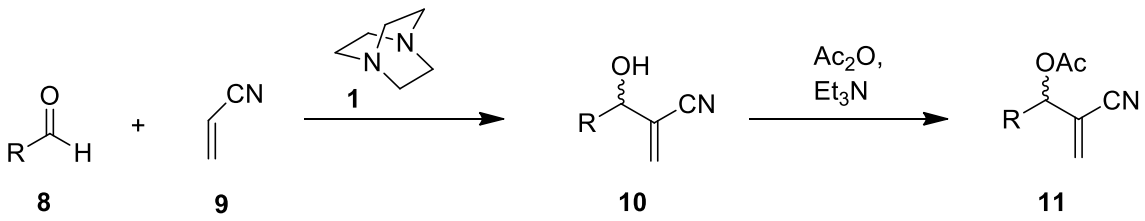
## 3.6. Enzyme Assay

Lipase activity was assayed by a method done using *p*-nitrophenyl esters, that is, *p*-nitrophenyl acetate, *p*-nitrophenyl butyrate, *p*-nitrophenyl caprylate and *p*-nitrophenyl palmitate as

substrates. The method involves measuring micromoles of *p*-nitrophenol (*p*-NP) released from *p*-nitrophenyl esters. An aliquot 20 µl of the substrate stock solution (*p*-NP ester, 10 mM in HPLC grade acetonitrile) was added into 960 µl of Tris-HCl (20 mM, pH 8). To make final volume to 1 ml, 20 µl of the purified enzyme was added to initiate the reaction and incubated at 45 °C for 20 minutes. A positive control (porcine lipase, 2 mg/ml) and a negative control (heat-inactivated in a boiling water-bath for 5 minutes), in duplicates, were also set up and incubated with each assay. Absorbance of the heat-inactivated lipase was subtracted from the absorbance of the corresponding test sample. Each of these test samples were performed in triplicate and mean values recorded. The product *p*-nitrophenol was detected using a spectrophotometer at 410 nm. The unknown concentration of *p*-nitrophenol released was determined from a prepared reference curve of *p*-nitrophenol. One unit of lipase hydrolase activity was defined as the amount of enzyme releasing 1 µmol of *p*-nitrophenol released per minute at 45 °C.

## 3.7 Morita-Baylis-Hillman Reaction

The reagents and solvents were obtained from commercial suppliers. Solvents that were used for chromatographic separation were distilled before use. Reactions were monitored using TLC (thin layer chromatography) on aluminium-backed Merck silica gel 60 $F_{254}$ plates. Separation of compounds by column chromatography was performed on normal silica gel (particle size 0.063-0.200 mm) or flash silica gel (particle size 0.040-0.063 mm) purchased from Merck. The $^{1}H$ NMR and $^{13}C$ NMR spectra were recorded on Bruker AVANCE 300 MHz and 400 MHz spectrometers. Spectra were recorded in deuterated chloroform. The chemical shift values for all spectra obtained are reported in parts per million and referenced against a standard, TMS, which occurs at zero parts per million. Coupling constants are given in Hertz. The Morita-Baylis-Hillman adducts, and corresponding acetates were prepared according to **Scheme 3.1**.




**a** R = Ph
**b** R = $PhCH_2CH_2$-

**Scheme 3. 1**: Preparation of Morita-Baylis-Hillman adducts **10** and acetates **11**. The aldehyde (**8**) is mixed with acrylonitrile (**9**) and the reaction is catalysed by DABCO (**1**). Acetylation is done using triethylamine and acetic anhydride.

## 3.7.1 Column Chromatography

A typical column involves a stationary phase and a mobile phase. The stationary phase is a solid adsorbent, normally silica gel ($SiO_2$), placed in a vertical glass column. The mobile phase is a liquid, added to the top of the column that flows down through the column by either gravity or external pressure (flash chromatography). Separation of compounds is achieved through the varying adsorption on, and interaction between, the compound and the stationary and mobile phases.

### 3.7.1.1 Column Preparation

A non-fritted column was used and plugged with cotton wool. The cotton wool was securely positioned in the narrowest part of the column using a long glass rod. The column was then clamped and filled about one fifth with solvent (20% ethanol/hexane). The required amount of silica gel was measured into a beaker. In a separate beaker, solvent, approximately one and a half times the volume of silica was measured. The silica was added to the solvent, a little at a time, while swirling. The slurry was then poured into the column, with solvent allowed to drip. The column was gently tapped to allow the silica to settle. The column sides were rinsed with solvent by pipetting solvent down the inside edge. A layer of sand (3 mm) was then added on top of the silica gel to prevent it from moving during solvent addition.

### 3.7.2 Synthesis of (±)-2-[(hydroxyphenyl)methyl]acrylonitrile 10a

A mixture of benzaldehyde **8a** (10.45 g, 0.098 mol), acrylonitrile **9** (40 mL, 0.608 mol) and DABCO **1** (10.9 g, 0.098 mol) were stirred at 0 °C for 19 h. After reaction completion, ethyl acetate (50 ml) and water (50 ml) were added to the reaction mixture and transferred into a 250 ml separating funnel. The mixture was vigorously shaken and allowed to settle. The organic layer was separated, dried over $MgSO_4$, solvent was removed *in vacuo* and the product **10a** was purified by column chromatography (20 % ethyl acetate/hexane).

### 3.7.3 Synthesis of (±)-2-cyano-1-phenylallyl acetate 11a

Triethylamine (3 mL, 0.040 mol), acetic anhydride (2 mL, 0.040 mol), and DMAP (24.28 mg, 0.199 mmol) were added to a stirred solution of (±)-2-[(hydroxyphenyl)methyl]acrylonitrile **10a** (3.16 g, 0.020 mol) in dichloromethane (25 ml). The resulting mixture was stirred at 25 °C for 30 minutes. An aqueous saturated solution of $NaHCO_3$ (50 ml) was added to the reaction mixture in a separating funnel and shaken. The organic layer was separated and dried using $MgSO_4$ and then concentrated *in vacuo*. The product **11a** was purified by column chromatography (20 % ethyl acetate/hexane).

### 3.7.4 Synthesis of (±)-3-hydroxy-2-methylene-5-phenylpentanenitrile 10b

The procedure used to synthesise (±)-2-[(hydroxyphenyl)methyl]acrylonitrile **10a** was used to synthesise (±)-3-hydroxy-2-methylene-5-phenylpentanenitrile **10b**, starting from **8b** and **9** in the presence of **1**. The reaction time was changed to 6 days. Purification was done by column chromatography.

### 3.7.5 Synthesis of (±)-2-cyano-5-phenyl-pent-1-ene-yl acetate 11b

The same procedure used to synthesise (±)-2-cyano-1-phenyl allyl acetate **11a** was used to synthesise (±)-2-cyano-5-phenyl-pent-1-ene-yl acetate **11b**, starting from compound **10b**.

## 3.8 Enzymatic Hydrolysis of Morita-Baylis-Hillman acetates

A Qubit® 2.0 fluorometer was used to determine the recombinant protein concentration. Four 20 ml push-on cap vials labelled 1 to 5 were set up in triplicate. Into the labelled 20 ml push-on cap vial, 10 mg/ml of the substrate was added and dissolved in acetone (20 % v/v). Thereafter, 3990 µl of 20 mM Tris-HCl (pH 8) containing crude enzyme extract was added to the vial labelled 1. An aliquot 10 µl of 0.05 mM calcium chloride was also added to the vial. Into a vial labelled 2, 4000 µl of 20 mM Tris-HCl (pH 8) containing crude enzyme extract and no calcium chloride was added. Into a vial labelled 3, 3990 µl of 20 mM Tris-HCl (pH 8) containing partially purified rPFL was added together with 10 µl of 0.05 mM calcium chloride. Into a vial labelled 4, 4000 µl of 20 mM Tris-HCl (pH 8) containing partially purified rPFL was added. Calcium chloride was not added. Into a vial labelled 5, 3990 µl of 20 mM Tris-HCl (pH 8) buffer with no enzyme and 10 µl of 0.05 mM calcium chloride. The resulting mixtures were incubated at 40 °C for 48 hours in an orbital shaker.

The reactions were stopped by adding 1 ml of 100 % (w/v) trichloroacetic acid (TCA) to precipitate the protein and were centrifuged at 14000 rpm for 5 minutes. The product, in the supernatant, was extracted using liquid-liquid extraction (ethyl acetate-water) in a separating funnel and concentrated on a rotary evaporator. The sample was run on a TLC plate with the starting material and alcohol derivative as controls. Concentrated reaction material was separated using column chromatography in a 50 ml syringe. Fractions for the different spots were pooled and concentrated *in vacuo*. Samples were analysed by NMR spectroscopy to confirm the structures of the compounds.

# 4 RESULTS

## 4.1 Transformation

The pET11a plasmid was successfully transformed into the JM109 cells. After transformation, plasmid extraction and restriction digest were conducted to confirm the presence of the plasmid. Restriction digest samples were run on agarose gel electrophoresis (Figure 4.1).

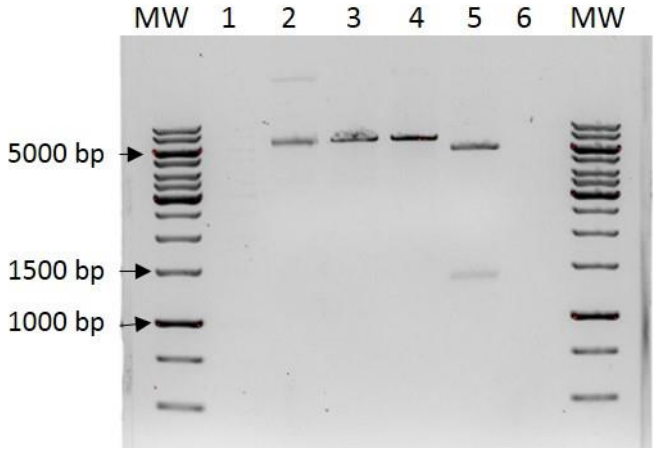



**Figure 4. 1**: Agarose gel electrophoresis of extracted pET11a plasmid from JM109 cells. An aliquot of 5 µl of the restriction digest samples were loaded on the gel. MW represented the molecular weight marker 1 Kb. On lane 2, undigested plasmid was loaded; lane 3 was loaded with BamHI digested plasmid; lane 4 with NdeI digested plasmid and lane 5 with double digested plasmid (BamHI and NdeI). Plasmid size = 5675 bp; Gene of interest size = 1359 bp.

Extracted pET11a plasmid was then successfully transformed into BL21 (DE3) pLysS, extracted and run on the agarose gel for confirmation (Figure 4.2).

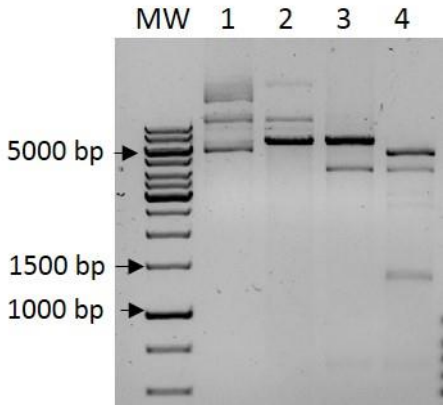



**Figure 4. 2:** Agarose gel electrophoresis of extracted pET11a plasmid from BL21 (DE3) pLysS cells. An aliquot of 5 µl of the restriction digest samples were loaded on the gel. MW represented the molecular weight marker 1 Kb. On lane 1, undigested plasmid was loaded; lane 2 was loaded with BamHI digested plasmid; lane 3 with NdeI digested plasmid and lane 4 with double digested plasmid (BamHI and NdeI). Plasmid size = 5675 bp; Gene of interest size = 1359 bp.

## 4.2 Expression Trials

Expression trials were conducted to identify the desirable conditions for expression. The *P. fluorescens* P26504 LipA_Psefl gene expressed at all four temperatures (20, 25, 30 and 37 °C). Expression levels varied with respect to temperature, IPTG concentration and time. At temperatures of 25 °C, 30 °C and 37 °C the protein was successfully expressed. High expression was observed to be greater at 25 °C, 1 mM IPTG and at 16 hours of expression (Figure 4.3).

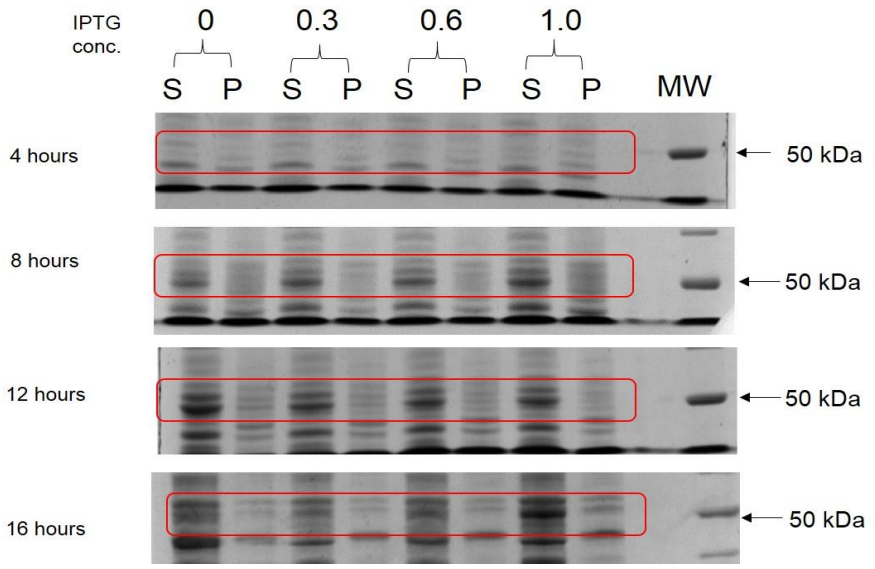



**Figure 4. 3:** SDS-PAGE analysis of the expression trial at 25 °C. The pET11a plasmid containing the *Pseudomonas fluorescens* lipase gene expressed in *E. coli* BL21 (DE3) pLySs. MW represents the PageRuler Unstained Protein Ladder(10-200kDa), P represent the resuspended pellet and S represents the supernatant. The protein (48.2 kDa) was not expressed at 4 hours. Protein expression in a soluble form seen from 8 hours to 16 hours, with high expression at 1mM IPTG concentration. (as shown in the red box).

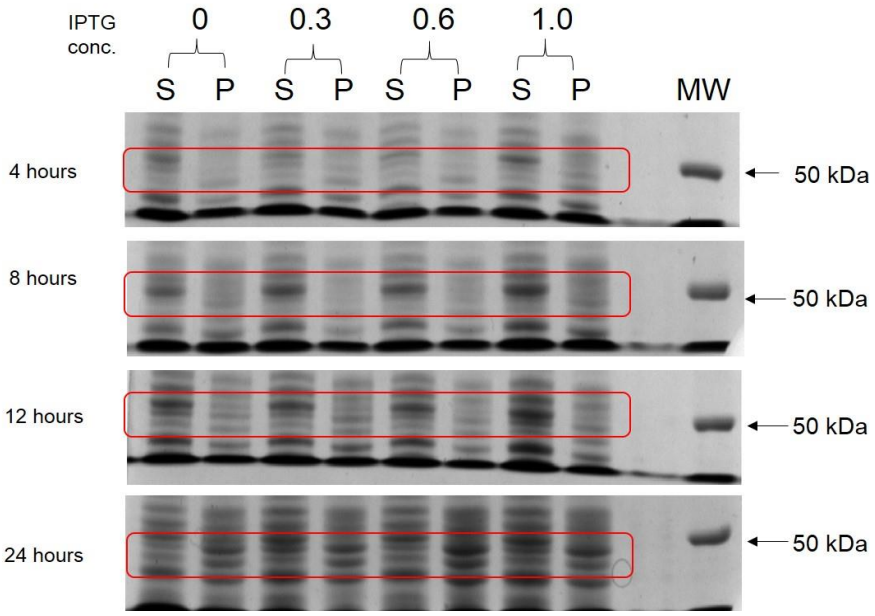



**Figure 4. 4:** SDS-PAGE analysis of the expression trial at 30 °C. The pET11a plasmid containing the *Pseudomonas fluorescens* lipase gene expressed in *E. coli* BL21 (DE3) pLySs. MW represents the PageRuler Unstained Protein Ladder(10-200kDa), P represent the resuspended pellet and S represents the supernatant. The protein (48.2 kDa) was not expressed at 4 hours. Protein expression in a soluble form seen from 8 hours to 16 hours, with high expression at 1mM IPTG concentration. At 24 hours, it was insoluble (as shown in the red box).

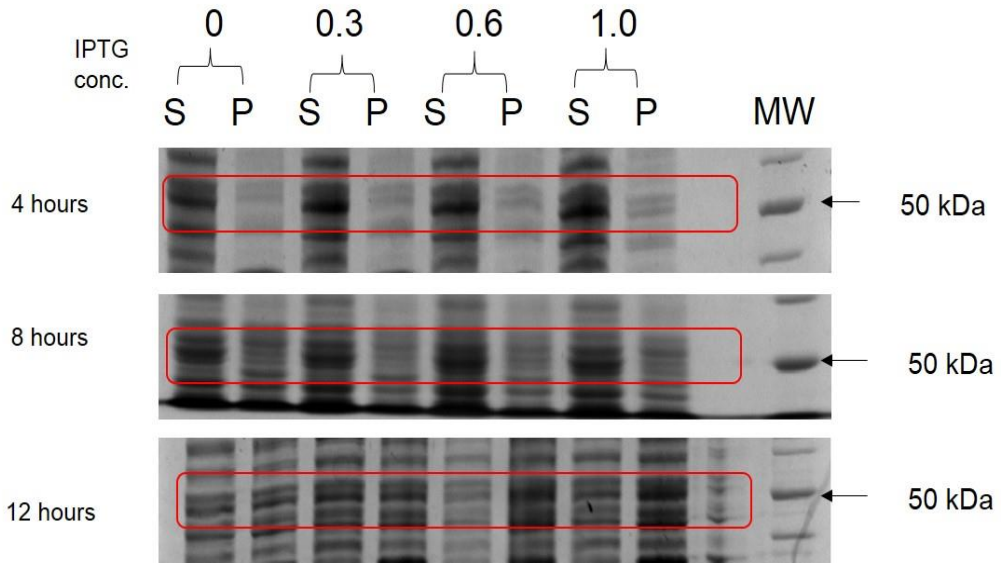



**Figure 4. 5:** SDS-PAGE analysis of the expression trial at 37 °C. The pET11a plasmid containing the *Pseudomonas fluorescens* lipase gene expressed in *E. coli* BL21 (DE3) pLySs. MW represents the PageRuler Unstained Protein Ladder(10-200kDa), P represent the resuspended pellet and S represents the supernatant. High expression in the supernatant seen at 4 hours and 8 hours. Expression at 12 hours was in the pellet form. Protein indicated as dark bands at close to 50 kDa mark (as shown in the red box).

## 4.3 Overexpression and Partial Purification

Heterologous overexpression was done at 25°C for 16 hours. Cells were resuspended in 20 mM Tris-HCl, pH 8, sonicated and centrifuged twice before loading the sample on the 5 ml DEAE column attached to the Äkta Prime Plus. Elution of the protein was done using a 0 to 1 M NaCl gradient over 20 mM Tris-HCl, pH 8. Figure 4.6 below shows the elution profile of the enzyme.

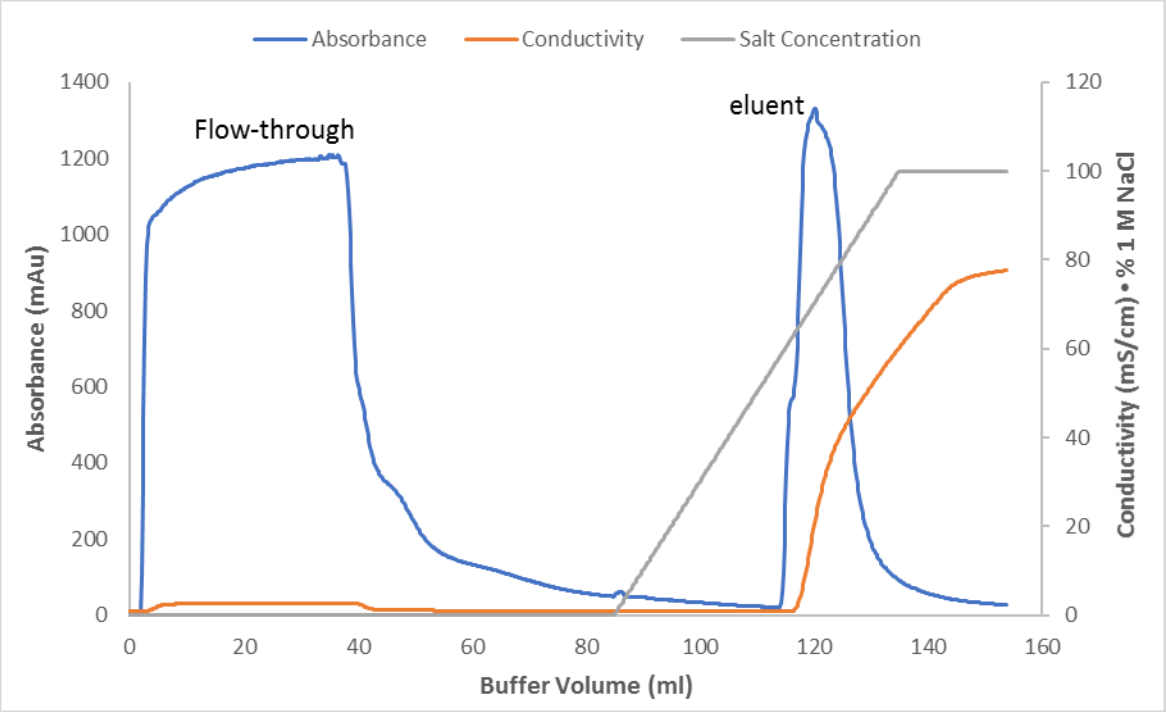



**Figure 4. 6:** Elution chromatogram of the recombinant *Pseudomonas fluorescens* lipase. The blue line represents absorbance of the supernatant, orange represents conductivity and the grey line represents the salt concentration at a linear gradient.

SDS-PAGE analysis was conducted on all the fractions collected from the Äkta Prime Plus to identify the presence of the recombinant *P. fluorescens* lipase. The darker band that was present closer to the 50 kDa mark showed the presence of the recombinant *P. fluorescens* lipase (Figure 4.7).

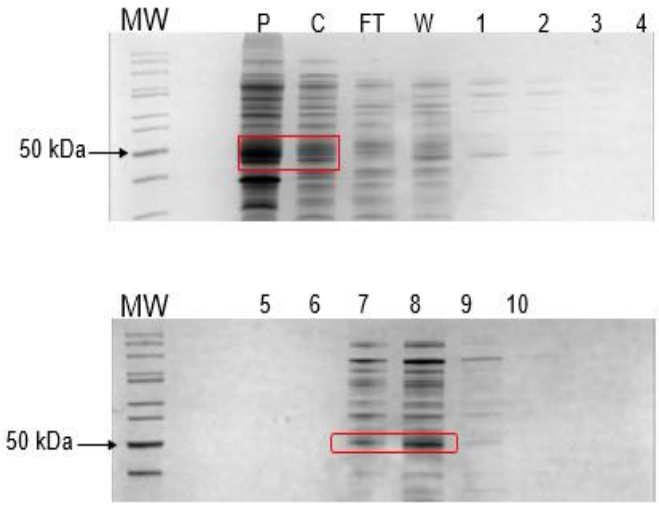



**Figure 4. 7:** SDS-PAGE analysis of the lipase expressed in *E. coli* and purified on the Akta Prime Plus using the HiTrap DEAE Sepharose FF column. MW represents the PageRuler Unstained Protein Ladder, P represents the resuspended pellet after sonication (with presence of protein in the red box), C represents the supernatant after sonication and centrifugation (also referred to as the crude), FT represents the flow through during purification, W represents the column wash after binding the protein to the column and numbers 1 to 10 are the different fractions collect with number 7 and 8 showing where the protein eluted (red box). The size of the lipase was 48.2 kDa.

## 4.4 Enzyme Assays

The lipase enzyme assays were conducted to further confirm the presence of the *P. fluorescens* lipase by checking whether it was in its active form or not. A 4-nitrophenol (*p*NP) standard curve was done to determine the amount of *p*NP released (Figure 4.8). Four *p*-nitrophenyl esters were prepared, that is, *p*-nitrophenyl acetate, *p*-nitrophenyl butyrate, *p*-nitrophenyl caprylate and *p*-nitrophenyl palmitate. Total Activity (U) was defined as the amount of enzyme required to produce 1 µmol of *p*-nitrophenol per minute at 410 nm. Specific Activity (U/mg) was calculated on each of the substrates as shown in Table 4.1 below.

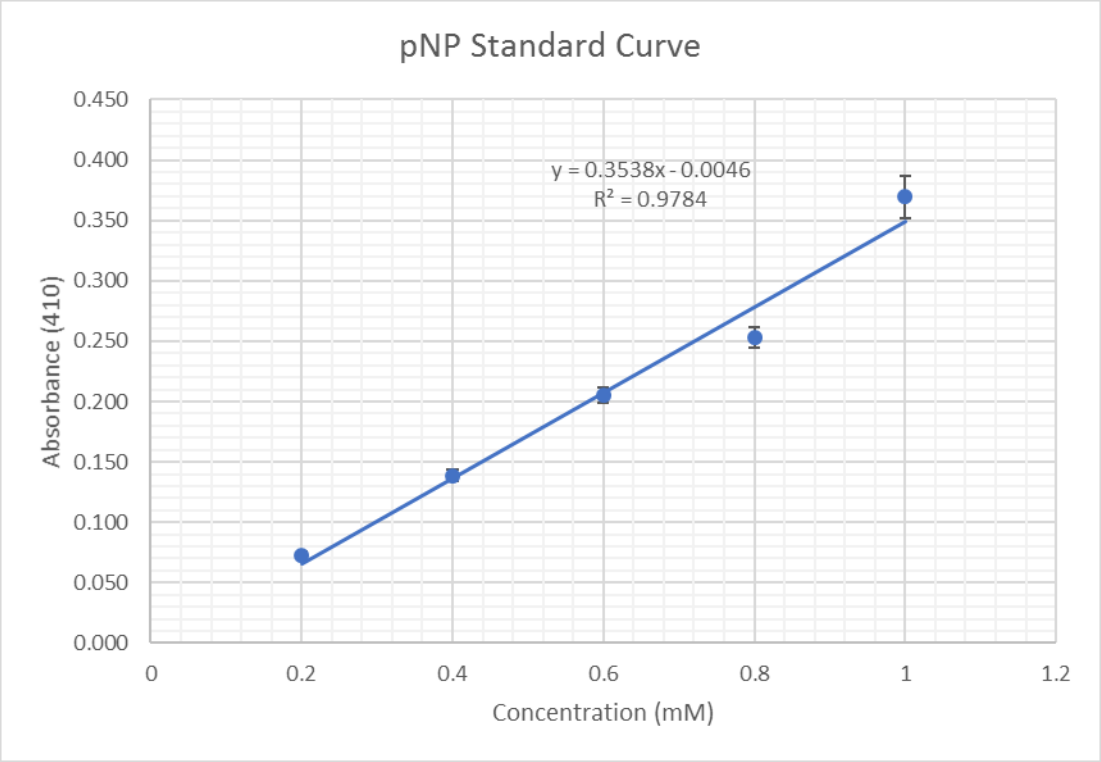



**Figure 4. 8:** Standard curve used to determine the rPFL activity based on the amount of *p*-nitrophenol liberated during the reaction.

**Table 4. 1:** Lipase activity measured using *p*-nitrophenyl esters.

| Substrate | Absorbance | *p*NP released (µmol) | Total (U) | Activity | Specific Activity (U/mg) |
|---|---|---|---|---|---|
| ***p*-Nitrophenyl acetate** | 0.648 | 1817 | 90.85 | | 55.73 |
| ***p*-Nitrophenyl butyrate** | 0.321 | 913 | 45.65 | | 28.01 |
| ***p*-Nitrophenyl caprylate** | 0.064 | 203 | 10.15 | | 6.23 |
| ***p*-Nitrophenyl palmitate** | 0.087 | 266 | 13.30 | | 8.16 |

## 4.5 Morita-Baylis-Hillman Adducts

The Morita-Baylis-Hillman reaction was conducted, giving rise to the Morita-Baylis-Hillman adducts. These compounds were then acetylated under standard conditions (as mentioned in the methods and materials section) and Morita-Baylis-Hillman acetates were obtained.

### 4.5.1 Synthesis of (±)-2-cyano-1-phenylallyl acetate 11a

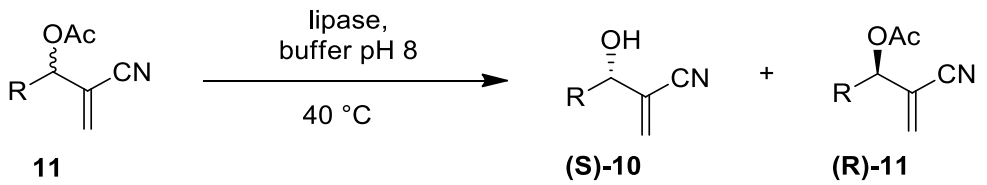
The desired product **11a** was purified by column chromatography and was afforded as a colourless oil (3.32 g, 94 %). $R_f$ = 0.59 (40% ethyl acetate/hexane); IR (neat, $cm^{-1}$) 3000, 2229, 1745, 1371, 1217; $^1$H NMR (400 MHz, $CDCl_3$) δ 7.42 - 7.35 (m, 5H), 6.33 (t, *J* = 1.3, 1.3 Hz, 1H),6.08 (d, *J* = 1.1 Hz, 1H), 6.00 (d, *J* = 1.3 Hz, 1H), 2.18 (s, 3H); $^{13}$CNMR (101 MHz, $CDCl_3$) δ 169.3, 135.6, 132.0, 129.2, 129.0, 127.0, 123.3, 116.2, 74.4, 21.0.

### 4.5.2 Synthesis of (±)-2-cyano-5-phenyl-pent-1-ene-yl-acetate 11b

The desired product **11b** was purified by column chromatography and was afforded as a colourless oil (3.91 g, 96 %). $R_f$ = 0.52 (40% ethyl acetate/hexane); IR (neat, $cm^{-1}$) 2937, 2227, 1742, 1454, 1371, 1220; $^1$H NMR (400 MHz, $CDCl_3$) δ 7.32-7.15 (m, 5H), 6.06 (s, 1H), 5.98 (d, *J* = 1.0 Hz, 1H), 5.28 (dd, *J* = 7.9, 5.9Hz, 1H), 2.67 (t, *J* = 7.9Hz, 2H), 2.10 (s, 3H); $^{13}$CNMR (101 MHz, $CDCl_3$) δ 169.9, 140.0, 133.0, 128.6, 128.3, 126.4, 122.6, 116.1, 72.7, 34.4, 31.2, 20.9.

## 4.6 Enzymatic Hydrolysis

The substrate (10 mg/ml) was added to the recombinant *P. fluorescens* lipase in 20 mM Tris-HCl, pH 8. The reaction mixture was incubated at the specified temperature and monitored for 48 hours. The reaction hydrolysis reaction is shown in Scheme 4.1.




**11** **(S)-10** **(R)-11**

**a** R = Ph
**b** R = $PhCH_2CH_2$-

**Scheme 4. 1**: Enzymatic hydrolysis of Morita-Baylis-Hillman acetates.

The reaction was stopped, protein precipitated using TCA and compounds extracted using liquid-liquid extraction. The compounds were concentrated *in vacuo* to afford a colourless oil (~8 mg). TLC analysis of the hydrolysis reaction showed the presence of two spots, corresponding to acetate 11a and alcohol 10a, showing that enzymatic hydrolysis of the acetate had occurred (Figure 4.9).

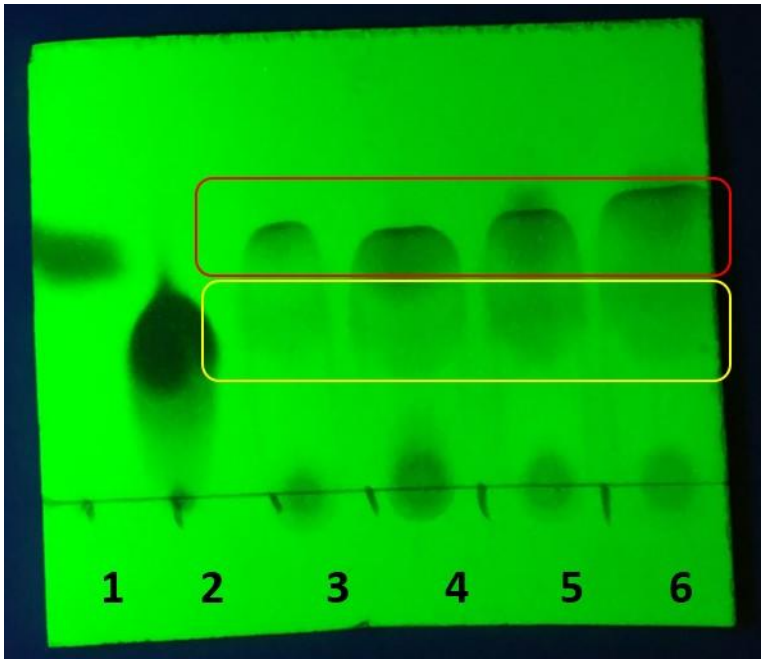



**Figure 4. 9:** TLC plate under UV showing the hydrolysis of the substrate (±)-2-cyano-1-phenyl allyl acetate **11a**. Spot number 1 represents the starting material **10a**; spot number 2 represents the alcohol derivative, **10a**; spot number 3 represents the substrate hydrolysed by the crude enzyme extract; spot 4 is the substrate with crude enzyme extract with calcium ions; spot 5 represents the substrate hydrolysed by the recombinant *P. fluorescens* lipase in the presence of calcium ions and spot 6 represents hydrolysis of the substrate by the recombinant *P. fluorescens* with no calcium ions. Highlighted in Red are the spots corresponding to the starting material and in Yellow corresponding to the alcohol derivative.

Enzymatic hydrolysis of substrate **11b** was also successful and the reaction showed two distinct spots corresponding to acetate **11b** and alcohol **10b** when spotted on the TLC plate (Figure 4.10)

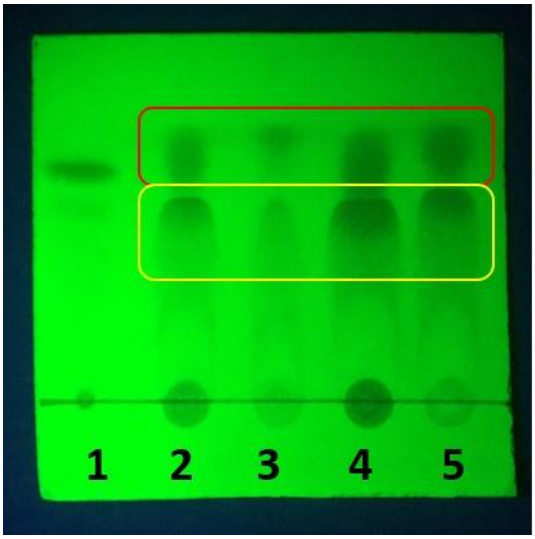



**Figure 4. 10:** TLC plate under UV showing the hydrolysis of the substrate (±)-2-cyano-5-phenyl-pent-1-ene-yl acetate **11b**. Spot number 1 represents the starting material **11b** and a faint spot for product **10b**; spot number 2 represents the substrate hydrolysed by the crude enzyme extract with calcium ions; spot 3 is the substrate with crude enzyme extract; spot 4 represents the substrate hydrolysed by the recombinant *P. fluorescens* lipase in the presence of calcium ions and spot 5 represents hydrolysis of the substrate by the recombinant *P. fluorescens* lipase with no calcium ions. Highlighted in Red are the spots corresponding to the starting material and in Yellow corresponding to the alcohol derivative.

# 5 DISCUSSION

## 5.1 Transformation

The pET11a plasmid harbouring the gene sequence coding for the *P. fluorescens* lipase (LIPA_pET11a), from GenScript Inc. was transformed into JM109 cells. The pET11a plasmid vector has a gene coding for ampicillin resistance which enables it to grow in the presence of the antibiotic ampicillin. After transformation, the cells were grown at 37 °C overnight in 2YT agar supplemented with 100 µg/ml ampicillin. Growth on the plates indicated only the successfully transformed cells. Plasmid extraction was conducted to further confirm the presence of the LIPA_pET11a. Enzyme restriction digest was done using BamHI and NdeI to separate the gene of interest (P26504 LIPA-Psefl, 1359 bp) from cloning vector (pET11a, 5675 bp). Enzyme restriction digest is a technique used in molecular biology to allow DNA analysis on techniques such as agarose gel electrophoresis. Restriction enzymes recognise one or a few target sequences on the DNA/plasmid molecule, thereby cleaving at those points (Gowland, 1994). The agarose gel electrophoresis (Figure 4.1) conducted showed the presence of the undigested LIPA_pET11a band at just above 6000 bp. The single digest bands also appeared above 6000 bp, showing that the gene of interest was still attached to the now linear plasmid. Double digested plasmid bands appeared at 5000 bp and closer to 1500 bp corresponding to the vector and the gene of interest. The gels obtained corresponded to the GenScript Certificate of Analysis (Project ID: U6644CE080-3).

Extracted plasmid from the JM109 cells was successfully transformed into the BL21 (DE3) pLysS competent cells. The analysis of the agarose gel electrophoresis of the extracted and enzyme digested plasmid (Figure 4.2) showed a similar result to that of the JM109 cells. However, some bands also appeared in the gels at just below 5000 bp. BL21 (DE3) pLysS cells contain a pLysS plasmid which produces a T7Lys inhibitor. The T7Lys inhibits the T7 RNA polymerase, hence avoiding toxicity caused by a leaky expression (Wagner *et al.*, 2008). The plasmid extraction kit is not specific thereby removes all the plasmids that are present in the cells. The pLysS plasmid is 4886 bp in size and contains a BamHI restriction site. This explains the presence of the band on lane 3 and 4 in the gel (Figure 4.2).

## 5.2 Expression Trials and Overexpression

Recombinant protein production has become a major technique in biotechnology. Bacterial expression systems have been intensively characterised and *E. coli* bacterial strains the most commonly used. Overexpression in *E. coli* cells is preferred because *E. coli* has a high cell density and is cost effective. Recombinant lipases, such as *Pseudomonas fluorescens* SIK W1, *P. moraviensis* M929, and *Pseudomonas* sp. R0–1430, are expressed in *E. coli* cells as inclusion bodies. Excessive rapid expression has been found to be the cause of formation of inclusion bodies of these recombinant proteins. The BL21 (DE3) pLysS cells were used to express the P26504 LipA_Psefl gene (Baneyx, 1999; Terpe, 2006). There was no previous study on this particular gene which provided the expression conditions of these gene coding for the *P. fluorescens* lipase, hence expression trials were conducted to try and determine an optimal expression strategy (Schlegel *et al*., 2010). Expression trials were done at 20-, 25-, 30- and 37 °C. SDS-PAGE analysis corresponded with the theoretical mass which was 48.2 kDa, determined using ProtParam.

Recombinant protein expression at 25 °C (Figure 4.3) was seen after 8 hours of induction. At 4 hours no recombinant protein expression was detected. At 8 hours and 12 hours, there was a fair amount of recombinant protein expressed. SDS-PAGE analysis of the expression trial at 25 °C for 16 hours showed that the protein expressed in high quantities in the presence of 1 mM IPTG. Figure 4.3 also showed some leaky expression with some protein expression taking place in the absence of IPTG. Other concentrations also showed a reasonable amount of expression of the protein as indicated in Figure 4.3 (Wagner *et al*., 2008). Recombinant protein expression at 30 °C (Figure 4.4) showed good recombinant protein at 8 hours and 12 hours. However, at 24 hours the recombinant protein was found to exist in the pellet form. This suggested that at 30 °C, the recombinant protein tends to form inclusion bodies after 24 hours. Expression at 37 °C showed the formation of inclusion bodies after 12 hours of induction (Figure 4.5).

The expression trials were an indication and validation of previous studies on *Pseudomonas* lipases being expressed at low temperatures. A study on *P. fluorescens* Pf0–1 showed that the expression of the recombinant protein in BL21 (DE3) pLysS occurred after induction at low temperature, with the recombinant protein being overexpressed in a soluble and catalytically active form (Liu *et al*., 2017). The *E. coli* strain BL21 (DE3) pLysS strain contains T7 RNA polymerase gene that is repressed by *lac*I. The *lac*I is relieved in the presence of an inducer,

isopropyl β-D-1-thiogalactopyranoside (IPTG). IPTG binds to the *lac* repressor and releases the tetrameric repressor, hence allowing transcription to occur. The recombinant protein of interest also expressed in the soluble fraction. Studies have shown that there are a limited number of proteins expressed in the soluble fraction and those being from *P. fragi* IFO 34584, *P. fluorescens* C9 and *P. fluorescens* JCM5963 (Zhang *et al*., 2009). The protein of interest, *P. fluorescens* P26504 had characteristics of subfamily I.3 *Pseudomonas* lipases with a molecular weight of 48.2 kDa. In general, these lipases have been found not to require the aid of a lipase-specific foldase (Lif) for them to be expressed in active forms (Aripigny and Jaeger, 1999). Their expression is in very low concentrations.

## 5.3 Partial Purification

Recombinant protein purification has been done not only to isolate the lipase enzymes from contaminants but also to assist in improving their activity and stability. The recombinant *P. fluorescens* P26504 lipase was partially purified using ion exchange chromatography on the Äkta Prime Plus. Ion exchange chromatography is based on the binding of charged sample proteins to charged groups attached onto an insoluble matrix. Ion exchangers such as the diethylaminoethyl (DEAE) group, and the cation exchangers based on the carboxymethyl (CM) group are widely used for protein purification (Saxena *et al*., 2003).

Buffer preparation was based on the isoelectric point (pI) of the protein (8.4) and also on the type of ion exchanger. Previous purification profiles done in the lab in a separate project by Padi, (2017), showed that the recombinant *P. fluorescens* P26504 (protein of interest) could not bind to the CM column. The CM column had been selected as the column of choice because cation exchangers require a buffer at least 1 pH unit below the pI of the protein to be bound and anion exchangers require a buffer which is at least 1 pH unit above the pI. The user manual for the columns stated that the ideal pH for anion exchanger was in the range of pH 7.6 – 8.6 when used with Tris-HCl buffer. The buffer of choice was 20 mM Tris-HCl pH 8, and the ion exchanger of choice was DEAE.

The purification profile (Figure 4.6) showed that the protein managed to bind to the column and an increase in salt gradient eluted the protein. A peak appeared at buffer volume of 115 ml to 135 ml. SDS-PAGE analysis (Figure 4.7) showed that the protein was present in both the

crude supernatant and the pellet. Only the crude was injected into the column and most of the protein of interest bound to the column as no protein of interest was detected in the flow-through. Small traces of the protein of interest were in the wash fraction. The fractions that corresponded to the peak area as seen on Figure 4.6 were collected as fraction 7 and 8. Fraction 8 showed a larger amount of the protein of interest compared to fraction 7 as shown in Figure 4.7.

## 5.4 Enzyme assays

Enzymes assays were conducted to check the activity of the partially purified recombinant *P. fluorescens* P26504 lipase. The study showed that the recombinant lipase exhibited activity towards *p*-nitrophenyl esters of different chain lengths at different rates. Table 3.1 shows that the lipase had the highest hydrolytic activity with $pNC_2$ with total activity of 90.85 U, with $pNC_4$ moderately high with total activity of 45.65 U. This demonstrated that the lipase prefers short-chain length fatty acids esters. Studies on other *Pseudomonas* lipases showed that they preferred medium-length fatty acid esters (Zhang *et al*., 2009). Activity was higher with $pNC_{16}$ as compared to $pNC_8$. Assays were repeated trying to eliminate handling error.

## 5.5 Morita-Baylis-Hillman Reaction

The Morita Baylis-Hillman reactions were performed on a small scale according to a study by Juma *et al.*, 2017. These reactions were monitored using thin layer chromatography. TLC is a chromatographic technique that is used to distinguish how many compounds are in a mixture. The compounds are spotted at the bottom of a TLC plate which is usually made of glass-, or aluminium and coated with silica. In this study, aluminium TLC plates coated with silica were used. Compounds that were being synthesised were not coloured hence the TLC plates were viewed under UV light. A retention factor (R*f*) value, which is defined as the distance travelled by the compound divided by the distance travelled by the solvent front, was calculated for each compound (Kowalska and Sherma, 2006).

## 5.5.1 Preparation of Morita-Baylis-Hillman adducts 10a and 10b

The reaction between benzaldehyde **8a** and acrylonitrile **9** gave rise to the Morita-Baylis-Hillman adduct **10a**. The reaction was stirred at 0 ° C for 19 hours. Compound was extracted using ethyl acetate and purified by column chromatography. The colourless oil that was afforded had an $R_f$ value of 0.51 on the thin layer chromatography (TLC) plates which corresponded to the $R_f$ value of 0.56 obtained by Juma *et al*., 2017. Nuclear Magnetic Resonance (NMR) analysis was also conducted but due to technical glitches, the proton NMR data of the compound was obtained without the required integrations. However, the NMR chemical shift values corresponded with what was achieved in Juma *et al*., 2017, hence allowing the continuation onto the next step of the reaction. Nuclear Magnetic Resonance (NMR) is an analytical technique that is used for molecular identifications. For quality control purposes, it can help in identifying the purity of a compound and also its molecular structure. Structures of compounds can be assigned based on integration, chemical shifts, spin multiplicity and coupling constants (Bruice, 2003; Hardinger, 2010).

The reaction between hydro-cinnamaldehyde **8b** and **9** gave rise to the Morita-Baylis-Hillman adduct **10b**. The reaction was left to stir for 6 days at 25 °C. The desired compound was extracted and purified by column chromatography. TLC results showed an $R_f$ value of 0.6 (40 % ethyl acetate/hexane), which was identical to the value obtained by Juma *et al*, 2017.

## 5.5.2 Preparation of Morita-Baylis-Hillman acetates 11a and 11b

The acetylation reaction on the adducts was done using acetic anhydride and triethylamine. Compound **11a** was obtained as a colourless oil with an $R_f$ value of 0.59 (40 % ethylacetate/hexane). Compound **11a** was obtained in a 94 % yield which was slightly higher than what was previously reported by Juma *et al*., 2017. Further characterisation was done by $^{1}H$ NMR and $^{13}C$ NMR spectroscopy. The $^{1}H$ NMR spectrum showed the presence of five aromatic protons in the region 7.42-7.35 ppm, which appeared as a multiplet. At 6.33 ppm, we observed one proton with a triplet splitting, corresponding to C*H*OAc. The alkene protons appeared at 6.08 and 6.00 ppm, each integrating for one proton. The acetate was also present, appearing as a singlet at a chemical shift of 2.18 ppm, integrating for three protons. The

$^{1}$H NMR data helped with proving the structure of **11a** showing the presence of all 11 protons. The $^{13}$C NMR data corresponded with that obtained by Juma *et al.*, 2017.

Compound **11b** was obtained as a colourless oil with an $R_f$ value of 0.52 (40% ethylacetate/hexane). Further characterisation was done by $^{1}$H NMR and $^{13}$C NMR. The $^{1}$H NMR spectrum showed the presence of five aromatic protons between the regions 7.32-7.15 ppm, as a multiplet. The alkene protons appeared at chemical shifts of 6.06 and 5.98 ppm, with each signal integrating for one proton. These alkene protons showed a similar trend of chemical shifts with those found in compound **11a**. The CH proton at the stereogenic centre (C*H*OAc) appeared at a chemical shift of 5.28 ppm. The aliphatic protons of compound **11b** adjacent to the aromatic ring appeared at a chemical shift of 2.67 ppm, showing the presence of two protons with a triplet splitting. The $CH_3$ of the acetate was also present, appearing as a singlet at a chemical shift of 2.10 ppm, integrating for three protons. Structural elucidation of **11b** was confirmed by the $^{1}$HNMR data obtained. The $^{13}$C NMR spectrum was also analysed and corresponded to the data obtained in the previous study. The yield of **11b** was slightly higher than what was reported previously at 96 % as compared to 91 % obtained by Juma *et al*., 2017.

## 5.6 Lipase Catalysed Kinetic Resolution

Morita-Baylis-Hillman adducts have been valuable intermediates in organic synthetic chemistry. However, MBH adducts are synthesised in racemic form, hence the need for establishing a kinetic resolution reaction in the synthesis of enantiopure MBH alcohols. Lipases have been widely used in organic synthetic chemistry to catalyse the resolution of MBH adducts (Xavier *et al*., 2014).

A study made by Juma *et al*., 2017, showed that amongst other lipases, the *P. fluorescens* (Sigma-Aldrich cat. No. 95608) exhibited high enantioselectivity on the MBH acetates. Kinetic resolution of the benzaldehyde derivative (**11a**) and the *trans*-cinnamaldehyde derivative was very high with enantiomeric excess of the product (alcohol) of 94 % and 93 %, respectively. Kinetic resolution of the hydro-cinnamaldehyde (**11b**) did not occur and they only reported two lipases showing high enantioselectivity. This enzyme, however, has been discontinued

from production by Sigma-Aldrich hence the expression and partial purification of the *P. fluorescens* P26504 lipase to catalyse the kinetic resolution.

Two substrates, benzaldehyde derivative (**11a**) and the hydro-cinnamaldehyde (**11b**) were successfully synthesised. Recombinant *P. fluorescens* P26504 lipase was partially purified to a concentration ranging between 1.5 mg/ml to 2.8 mg/ml. A substrate concentration of 10 mg/ml dissolved in acetone was added to the enzyme solution to start the kinetic resolution. Crude extract reactions were also set up and run in parallel with the partially purified lipase. The reactions were incubated at 40 °C for 48 hours. The reaction was stopped, and the protein precipitated using TCA. Compound extraction using ethylacetate was done, and then the compound was concentrated *in vacuo*.

Figure 4.10 shows TLC analysis of compound **11a**, with the starting material **10a**, the known alcohol, and the four reactions containing the recombinant lipase. In lane 3, the spot represents the crude enzyme extract that showed two different spots with one lighter spot corresponding to the known alcohol and the other darker spot corresponding to the starting material. Lane 4 showed the spots that represented catalysis by the crude enzyme extract that contained 0.05 M calcium chloride. The results were similar to lane 3 results showing that the enzymatic hydrolysis had occurred. In lane 5 and 6, we had spots representing the partially purified recombinant lipase with 0.05 M calcium ions and partially purified recombinant lipase without the calcium ions, respectively. The spot in lane 5 corresponding with the $R_f$ value of the alcohol was darker than the spot in lane 6, indicating that the best results occurred in the presence of calcium ions. This might also be explained by studies conducted on the effect of calcium ions on lipases, with reports showing that calcium ions play an important role in the structure and function of *Pseudomonas* lipases (Verma *et al*., 2012).

Figure 4.11 shows TLC analysis of compound **11b**, with the starting material **10b**, and the four reactions containing the recombinant lipase. The spot in lane 2 represents the substrate hydrolysed by the crude enzyme extract with calcium ions and the spot in lane 3 is the substrate with crude enzyme extract without the calcium ions. The spot corresponding to the $R_f$ value of the known alcohol was darker in lane 2 as compared to lane 3. The spot in lane 4 represents the substrate hydrolysed by the recombinant *P. fluorescens* lipase in the presence of calcium ions and spot in lane 5 represents hydrolysis of the substrate by the recombinant *P. fluorescens* lipase with no calcium ions. Once again, the hydrolysis reaction containing calcium ions seemed to represent the best conversion of starting material into product. The two spots in

lane 4 had an intensity that was similar. This implies that the enzyme was able to convert approximately 50 % of the starting material. In a successful kinetic resolution, the maximum theoretical yield is 50 % (Li *et al*., 2016). Although from TLC analysis alone it is not possible to determine if the hydrolysis is enantioselective, the fact that only 50 % conversion occurred is promising. A non-selective enzyme would convert all of the starting material into product. The result obtained for compound **11b** was of utmost interest as the previous study done by Juma *et al*., 2017 showed that kinetic resolution of the compound was challenging. In this case the enzyme was shown to have an approximately 50 % conversion of **11b**.

# 6 CONCLUSIONS

In this study, we successfully transformed the LIPA_pET11a coding for the *P. fluorescens* P26504 lipase into the *E. coli* expression systems JM109 and BL21 (DE3) pLysS. The recombinant lipase was expressed in a soluble and active form without the co-expression of a helper foldase. The recombinant lipase was also stable as it did not form aggregates during the partial purification and also during its application in the kinetic resolution. Enzyme assays using *p*-nitrophenyl esters, were also done to confirm the activity of the recombinant enzyme. The Morita-Baylis-Hillman reaction was conducted to produce two MBH adducts, that derived from benzaldehyde (**10a**) and the hydro-cinnamaldehyde derivative (**10b**). The MBH adducts were acetylated to give compounds **11a** and **11b,** respectively. Lipase-catalysed kinetic resolution was conducted on the MBH acetates using the partially purified recombinant lipase. TLC plate analysis showed that the recombinant *P. fluorescens* P26504 was able to hydrolyse both **11a** and **11b**. The fact that hydrolysis did not appear to proceed beyond 50 % is promising, as it may indicate that the hydrolysis was enantioselective. However, due to technical glitches, enantioselectivity could not be determined by HPLC analysis, which would be definitive. The compounds resulting from the hydrolysis reactions were separated using column chromatography, however, the concentration was too low for NMR analysis, and could not be fully characterised.

## 6.1 Recommendations

Future work needs to be done to confirm the enantioselectivity of *P. fluorescens* P26504 on the MBH acetates using chiral HPLC and calculating enantiomeric excess. The enantioselectivity confirmation can also be expanded by synthesizing a wide range of MBH substrates to be applied in the hydrolytic reaction. The lipase enzyme can also be further purified and characterised to increase its activity.

# 7 REFERENCES


Akbari, N., Khajeh, K., Rezaie, S., Mirdamadi, S., Shavandi, M. and Ghaemi, N., 2010. High-level expression of lipase in Escherichia coli and recovery of active recombinant enzyme through in vitro refolding. *Protein expression and purification*, *70*(1), pp.75-80.

Alba, A.N. and Rios, R., 2009. Kinetic resolution: a powerful tool for the synthesis of planar-chiral ferrocenes. *Molecules*, *14*(11), pp.4747-4757.

Alberghina, L., Schmid, R., and Verger, R. (Eds.). 1991. *Lipases: Structure, Mechanism, and Genetic Engineering: Contributions to the CEC-GBF International Workshop, September 13 to 15, 1990, Braunschweig, Germany* (Vol. 16). Braunschweig, Germany: VCH.

Alnoch, R.C., Stefanello, A.A., Martini, V.P., Richter, J.L., Mateo, C., de Souza, E.M., Mitchell, D.A., Muller-Santos, M. and Krieger, N., 2018. Co-expression, purification and characterization of the lipase and foldase of Burkholderia contaminans LTEB11. *International journal of biological macromolecules*, *116*, pp.1222-1231.

Andualema, B., and Gessesse, A. 2012. Microbial lipases and their industrial applications: review. *Biotechnology*, *11*(3), 100-118.

Angajala, G., Pavan, P., and Subashini, R. 2016. Lipases: An overview of its current challenges and prospectives in the revolution of biocatalysis. *Biocatalysis and Agricultural Biotechnology*, *7*, 257-270.

Arpigny, J.L. and JAEGER, K.E., 1999. Bacterial lipolytic enzymes: classification and properties. *Biochemical journal*, *343*(1), pp.177-183.

Baneyx, F., 1999. Recombinant protein expression in Escherichia coli. *Current opinion in biotechnology*, *10*(5), pp.411-421.

Bell, P. J., Sunna, A., Gibbs, M. D., Curach, N. C., Nevalainen, H., & Bergquist, P. L. (2002). Prospecting for novel lipase genes using PCRa. *Microbiology*, *148*(8), 2283-2291.

Bezborodov, A. M., and Zagustina, N. A. 2014. Lipases in catalytic reactions of organic chemistry. *Applied biochemistry and microbiology*, *50*(4), 313.

Bommarius, A. S., and Riebel-Bommarius, B. R. 2004. *Biocatalysis: fundamentals and applications*. John Wiley & Sons.

Bornscheuer, U. T., and Pohl, M. 2001. Improved biocatalysts by directed evolution and rational protein design. *Current opinion in chemical biology*, *5*(2), 137-143.

Bornscheuer, U.T., Bessler, C., Srinivas, R. and Krishna, S.H., 2002. Optimizing lipases and related enzymes for efficient application. *Trends in biotechnology*, *20*(10), pp.433-437.

Bruice, P.Y., 2003. *Organic chemistry 4 th edition* (Vol. 902). Pearson.

Burgess, K., and Jennings, L. D. 1990. Biocatalytic resolutions of. alpha.-methylene-. beta.-hydroxy esters and ketones. *The Journal of Organic Chemistry*, *55*(4), 1138-1139.

Davids, T., Schmidt, M., Böttcher, D. and Bornscheuer, U.T., 2013. Strategies for the discovery and engineering of enzymes for biocatalysis. *Current Opinion in Chemical Biology*, *17*(2), pp.215-220.

Davidson, S., 1996. Microbial lipases: production and applications. *Science progress*, *79*(2), pp.119-157.

Davranov, K. and Khalameizer, V.B., 1997. Current state of the study of microbial lipases. *Chemistry of natural compounds*, *33*(2), pp.113-126.

De Regil, R., and Sandoval, G. 2013. Biocatalysis for biobased chemicals. *Biomolecules*, *3*(4), 812-847.

Drauz, K. 2012. *Enzyme catalysis in organic synthesis: a comprehensive handbook*. John Wiley & Sons.

Facchin, S., Alves, P.D.D., de Faria Siqueira, F., Barroca, T.M., Victória, J.M.N. and Kalapothakis, E., 2013. Biodiversity and secretion of enzymes with potential utility in wastewater treatment. *Open Journal of Ecology*, *3*(1), p.34.

Ferrario, V., Ebert, C., Knapic, L., Fattor, D., Basso, A., Spizzo, P. and Gardossi, L., 2011. Conformational changes of lipases in aqueous media: A comparative computational study and experimental implications. *Advanced Synthesis & Catalysis*, *353*(13), pp.2466-2480.

Ghori, M.I., Iqbal, M.J. and Hameed, A., 2011. Characterization of a novel lipase from Bacillus sp. isolated from tannery wastes. *Brazilian Journal of Microbiology*, *42*(1), pp.22-29.

Gilbert, E.J., 1993. Pseudomonas lipases: biochemical properties and molecular cloning. *Enzyme and Microbial Technology*, *15*(8), pp.634-645.

Gilbert, E.J., Cornish, A. and Jones, C.W., 1991. Purification and properties of extracellular lipase from Pseudomonas aeruginosa EF2. *Microbiology*, *137*(9), pp.2223-2229.

Gowland, P.C., 1994. Determination of the molecular size of a plasmid following restriction endonuclease digestion. *Biochemical education*, *22*(2), pp.95-96.

Gupta, M.N., Batra, R., Tyagi, R. and Sharma, A., 1997. Polarity index: the guiding solvent parameter for enzyme stability in aqueous-organic cosolvent mixtures. *Biotechnology progress*, *13*(3), pp.284-288.

Gupta, R., Gupta, N., and Rathi, P. 2004. Bacterial lipases: an overview of production, purification and biochemical properties. *Applied microbiology and biotechnology*, *64*(6), 763-781.

Hardinger, S.A., 2010. *Chemistry 14C: Organic Molecular Structures and Interactions: PowerPoint Lectures for Chemistry 14C with PowerPoint CD*. Hayden-McNeil Pub.

Hasan, F., Shah, A. A., and Hameed, A. 2006. Industrial applications of microbial lipases. *Enzyme and Microbial technology*, *39*(2), 235-251.

Hayashi, N., Yanagihara, K., and Tsuboi, S. 1998. Lipase-catalyzed kinetic resolution of Baylis–Hillman products. *Tetrahedron: Asymmetry*, *9*(21), 3825-3830.

Henne, A., Schmitz, R. A., Bömeke, M., Gottschalk, G., and Daniel, R. 2000. Screening of Environmental DNA Libraries for the Presence of Genes Conferring Lipolytic Activity onEscherichia coli. *Applied and environmental microbiology*, *66*(7), 3113-3116.

Hertadi, R. and Widhyastuti, H., 2015. Effect of Ca2+ Ion to the Activity and Stability of Lipase Isolated from Chromohalobacter japonicus BK-AB18. *Procedia Chemistry*, *16*, pp.306-313.

Holmquist, M. 2000. Alpha beta-hydrolase fold enzymes structures, functions and mechanisms. *Current Protein and Peptide Science*, *1*(2), 209-235.

Houde, A., Kademi, A. and Leblanc, D., 2004. Lipases and their industrial applications. *Applied biochemistry and biotechnology*, *118*(1-3), pp.155-170.

Jaeger, K. E., and Eggert, T. 2002. Lipases for biotechnology. *Current opinion in biotechnology*, *13*(4), 390-397.

Jaeger, K. E., and Reetz, M. T. 1998. Microbial lipases form versatile tools for biotechnology. *Trends in biotechnology*, *16*(9), 396-403.

Jaeger, K. E., Ransac, S., Dijkstra, B. W., Colson, C., van Heuvel, M., & Misset, O. (1994). Bacterial lipases. *FEMS microbiology reviews*, *15*(1), 29-63.

Jaeger, K. E., Dijkstra, B. W., and Reetz, M. T. 1999. Bacterial biocatalysts: molecular biology, three-dimensional structures, and biotechnological applications of lipases. *Annual Reviews in Microbiology*, *53*(1), 315-351.

Javed, S., Azeem, F., Hussain, S., Rasul, I., Siddique, M.H., Riaz, M., Afzal, M., Kouser, A. and Nadeem, H., 2018. Bacterial lipases: a review on purification and characterization. *Progress in biophysics and molecular biology*, *132*, pp.23-34.

Juma, W.P., Chhiba, V., Brady, D. and Bode, M.L., 2017. Enzymatic kinetic resolution of Morita-Baylis-Hillman acetates. *Tetrahedron: Asymmetry*, *28*(9), pp.1169-1174.

Kanwar, S.S., Kaushal, R.K., Jawed, A., Gupta, R. and Chimni, S.S., 2005. Methods for inhibition of residual lipase activity in colorimetric assay: A comparative study.

Kazlauskas, R.J. and Bornscheuer, U.T., 1998. Biotransformations with lipases. *Biotechnology: Biotransformations I*, *8*, pp.36-191.

Kazlauskas, R.J., Weissfloch, A.N., Rappaport, A.T. and Cuccia, L.A., 1991. A rule to predict which enantiomer of a secondary alcohol reacts faster in reactions catalyzed by cholesterol esterase, lipase from Pseudomonas cepacia, and lipase from Candida rugosa. *The Journal of Organic Chemistry*, *56*(8), pp.2656-2665.

Kowalska, T. and Sherma, J. eds., 2006. *Preparative layer chromatography*. CRC Press.

Kumar, A., Dhar, K., Kanwar, S. S., and Arora, P. K. 2016. Lipase catalysis in organic solvents: advantages and applications. *Biological procedures online*, *18*(1), 2.

Langer, P., 2000. New strategies for the development of an asymmetric version of the Baylis–Hillman reaction. *Angewandte Chemie International Edition*, *39*(17), pp.3049-3052.

Lason, E. and Ogonowski, J., 2010. Lipase-characterization, applications and methods of immobilization.

Latip, W., Rahman, R.N.Z.R.A., Leow, A.T.C., Shariff, F.M. and Ali, M.S.M., 2016. Expression and characterization of thermotolerant lipase with broad pH profiles isolated from an Antarctic Pseudomonas sp strain AMS3. *PeerJ*, *4*, p.e2420.

Li, P., Hu, X., Dong, X.Q. and Zhang, X., 2016. Recent Advances in Dynamic Kinetic Resolution by Chiral Bifunctional (Thio) urea-and Squaramide-Based Organocatalysts. *Molecules*, *21*(10), p.1327.

Liebeton, K., Zacharias, A. and Jaeger, K.E., 2001. Disulfide Bond in Pseudomonas aeruginosalipase stabilizes the structure but is not required for interaction with its foldase. *Journal of bacteriology*, *183*(2), pp.597-603.

Liu, W., Li, M. and Yan, Y., 2017. Heterologous expression and characterization of a new lipase from Pseudomonas fluorescens Pf0–1 and used for biodiesel production. *Scientific reports*, *7*(1), p.15711.

Macrae, A. R., & Hammond, R. C. (1985). Present and future applications of lipases. *Biotechnology and Genetic Engineering Reviews*, *3*(1), 193-218.

Mateo, C. and Palomo, J., 2018. Asymmetric and Selective Biocatalysis.

Muralidhar, R.V., Chirumamilla, R.R., Marchant, R., Ramachandran, V.N., Ward, O.P. and Nigam, P., 2002. Understanding lipase stereoselectivity. *World Journal of Microbiology and Biotechnology*, *18*(2), pp.81-97.

Nascimento, M.G., Zanotto, S.P., Melegari, S.P., Fernandes, L. and Sá, M.M., 2003. Resolution of α-methylene-β-hydroxy esters catalyzed by free and immobilized Pseudomonas sp. lipase. *Tetrahedron: Asymmetry*, *14*(20), pp.3111-3115.

Nawani, N. and Kaur, J., 2000. Purification, characterization and thermostability of lipase from a thermophilic Bacillus sp. J33. *Molecular and cellular Biochemistry*, *206*(1-2), pp.91-96.

Padi, T. Overexpression and purification of Lipase A from Pseudomonas fluorescens for biocatalytic use. Honours. University of The Witswatersrand, Johannesburg, 2017.

Pencreac'h, G. and Baratti, J.C., 1996. Hydrolysis of p-nitrophenyl palmitate in n-heptane by the Pseudomonas cepacia lipase: a simple test for the determination of lipase activity in organic media. *Enzyme and Microbial Technology*, *18*(6), pp.417-422.

Peng, R., Lin, J. and Wei, D., 2010. Purification and characterization of an organic solvent-tolerant lipase from Pseudomonas aeruginosa CS-2. *Applied biochemistry and biotechnology*, *162*(3), pp.733-743.

Reddy, T.N. and Rao, V.J., 2018. Importance of Baylis-Hillman adducts in modern drug discovery. *Tetrahedron letters*.

Reetz, M. T. 2002. Lipases as practical biocatalysts. *Current opinion in chemical biology*, *6*(2), 145-150.

Rios, N.S., Pinheiro, B.B., Pinheiro, M.P., Bezerra, R.M., dos Santos, J.C.S. and Gonçalves, L.R.B., 2018. Biotechnological potential of lipases from Pseudomonas: sources, properties and applications. *Process biochemistry*.

Sangeetha, R., Arulpandi, I. and Geetha, A., 2011. Bacterial lipases as potential industrial biocatalysts: An overview. *Res J Microbiol*, *6*(1), pp.1-24.

Santarossa, G., Lafranconi, P.G., Alquati, C., DeGioia, L., Alberghina, L., Fantucci, P. and Lotti, M., 2005. Mutations in the "lid" region affect chain length specificity and thermostability of a Pseudomonas fragi lipase. *FEBS letters*, *579*(11), pp.2383-2386.

Sarmah, N., Revathi, D., Sheelu, G., Yamuna Rani, K., Sridhar, S., Mehtab, V. and Sumana, C., 2018. Recent advances on sources and industrial applications of lipases. *Biotechnology progress*, *34*(1), pp.5-28.

Saxena, R. K., Sheoran, A., Giri, B., & Davidson, W. S. (2003). Purification strategies for microbial lipases. *Journal of Microbiological Methods*, *52*(1), 1-18.

Schägger, H., 2006. Tricine–sds-page. *Nature protocols*, *1*(1), p.16.

Shaikh, I.R., 2014. Organocatalysis: key trends in green synthetic chemistry, challenges, scope towards heterogenization, and importance from research and industrial point of view. *Journal of Catalysts*, *2014*.

Schlegel, S., Klepsch, M., Gialama, D., Wickström, D., Slotboom, D.J. and De Gier, J.W., 2010. Revolutionizing membrane protein overexpression in bacteria. *Microbial biotechnology*, *3*(4), pp.403-411.

Schmidt, M., Larsen, D.M. and Stougaard, P., 2010. A lipase with broad temperature range from an alkaliphilic gamma-proteobacterium isolated in Greenland. *Environmental technology*, *31*(10), pp.1091-1100.

Schrag, J.D., Li, Y., Cygler, M., Lang, D., Burgdorf, T., Hecht, H.J., Schmid, R., Schomburg, D., Rydel, T.J., Oliver, J.D. and Strickland, L.C., 1997. The open conformation of a Pseudomonas lipase. *Structure*, *5*(2), pp.187-202.

Schulz, T., Pleiss, J. and Schmid, R.D., 2000. Stereoselectivity of Pseudomonas cepacia lipase toward secondary alcohols: a quantitative model. *Protein Science*, *9*(6), pp.1053-1062.

Sharma, R., Chisti, Y. and Banerjee, U.C., 2001. Production, purification, characterization, and applications of lipases. *Biotechnology advances*, *19*(8), pp.627-662.

Sharma, R., Soni, S.K., Vohra, R.M., Gupta, L.K. and Gupta, J.K., 2002. Purification and characterisation of a thermostable alkaline lipase from a new thermophilic Bacillus sp. RSJ-1. *Process Biochemistry*, *37*(10), pp.1075-1084.

Sheldon, R.A., Arends, I. and Hanefeld, U., 2007. *Green chemistry and catalysis*. John Wiley & Sons.

Shiloach, J., Kaufman, J., Guillard, A.S. and Fass, R., 1996. Effect of glucose supply strategy on acetate accumulation, growth, and recombinant protein production by Escherichia coli BL21 (λDE3) and Escherichia coli JM109. *Biotechnology and bioengineering*, *49*(4), pp.421-428.

Stoytcheva, M., Montero, G., Zlatev, R., A Leon, J. and Gochev, V., 2012. Analytical methods for lipases activity determination: A review. *Current Analytical Chemistry*, *8*(3), pp.400-407.

Strub, D.J., Garbos, A. and Lochynskia, S., 2017. Synthesis, lipase catalyzed kinetic resolution, and determination of the absolute configuration of enantiomers of the Morita-Baylis-Hillman adduct 3-hydroxy-2-methylenebutanenitrile. *Arkivoc*, *2*, pp.313-323.

Studier, F.W., Daegelen, P., Lenski, R.E., Maslov, S. and Kim, J.F., 2009. Understanding the differences between genome sequences of Escherichia coli B strains REL606 and BL21 (DE3) and comparison of the E. coli B and K-12 genomes. *Journal of molecular biology*, *394*(4), pp.653-680.

Svendsen, A., Borch, K., Barfoed, M., Nielsen, T.B., Gormsen, E. and Patkar, S.A., 1995. Biochemical properties of cloned lipases from the Pseudomonas family. *Biochimica et Biophysica Acta (BBA)-Lipids and Lipid Metabolism*, *1259*(1), pp.9-17.

Tan, S., Apenten, R.O. and Knapp, J., 1996. Low temperature organic phase biocatalysis using cold-adapted lipase from psychrotrophic Pseudomonas P38. *Food chemistry*, *57*(3), pp.415-418.

Terpe, K., 2006. Overview of bacterial expression systems for heterologous protein production: from molecular and biochemical fundamentals to commercial systems. *Applied microbiology and biotechnology*, *72*(2), p.211.

Thakur, S., 2012. Lipases, its sources, properties and applications: a review. *Int J Sci Eng Res*, *3*(7), pp.1-29.

Truppo, M.D., 2017. Biocatalysis in the pharmaceutical industry: the need for speed. *ACS medicinal chemistry letters*, *8*(5), pp.476-480.

Verma, N., Thakur, S. and Bhatt, A.K., 2012. Microbial lipases: industrial applications and properties (a review). *Int Res J Biol Sci*, *1*(8), pp.88-92.

Wagner, S., Klepsch, M.M., Schlegel, S., Appel, A., Draheim, R., Tarry, M., Högbom, M., Van Wijk, K.J., Slotboom, D.J., Persson, J.O. and De Gier, J.W., 2008. Tuning Escherichia coli for membrane protein overexpression. *Proceedings of the National Academy of Sciences*, *105*(38), pp.14371-14376.

Wang, X., Yu, X. and Xu, Y., 2009. Homologous expression, purification and characterization of a novel high-alkaline and thermal stable lipase from Burkholderia cepacia ATCC 25416. *Enzyme and microbial technology*, *45*(2), pp.94-102.

Winkler, M., Glieder, A. and Steiner, K., 2012. C–X Bond Formation: Hydroxynitrile lyases: From Nature to Application. In *Comprehensive chirality*. Elsevier BV.

Wu, X., You, P., Su, E., Xu, J., Gao, B. and Wei, D., 2012. In vivo functional expression of a screened P. aeruginosa chaperone-dependent lipase in E. coli. *BMC biotechnology*, *12*(1), p.58.

Xavier, F.J., Neto, J.S., Néris, P.L., Oliveira, M.R., Vale, J.A. and Vasconcellos, M.L., 2014. Kinetic resolution of leishmanicidal meta and para (±)-2-[Hydroxy (nitrophenyl) methyl] acrylonitrile catalyzed by CALB: In vitro evaluations of separated meta (R),(S) and (R/S) adducts. *Journal of Molecular Catalysis B: Enzymatic*, *108*, pp.7-12.

Yaacob, N., Ali, M.S.M., Salleh, A.B., Rahman, R.N.Z.R.A. and Leow, A.T.C., 2016. Toluene promotes lid 2 interfacial activation of cold active solvent tolerant lipase from Pseudomonas fluorescens strain AMS8. *Journal of Molecular Graphics and Modelling*, *68*, pp.224-235.

Yadav, J.S., Reddy, B.S., Basak, A.K. and Narsaiah, A.V., 2007. Microwave accelerated SN2′ substitution of Baylis–Hillman acetates: A comparative study of conventional heating versus microwave irradiation. *Journal of Molecular Catalysis A: Chemical*, *274*(1-2), pp.105-108.

Zhang, T. Z., Dai, L. X., & Hou, X. L. (2007). Enantioselective allylic substitution of Morita–Baylis–Hillman adducts catalyzed by planar chiral [2.2] paracyclophane monophosphines. *Tetrahedron: Asymmetry*, *18*(16), 1990-1994.

# Appendix

## A1 Molecular Weight Ladders

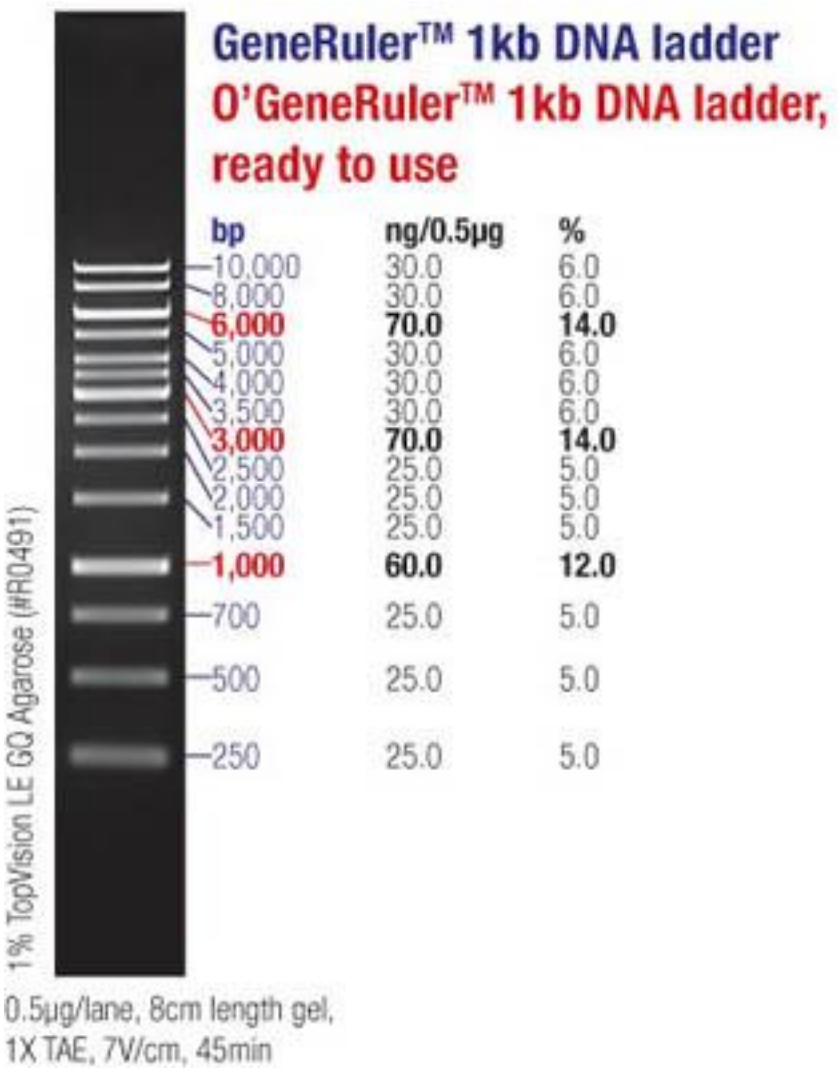



**Figure A1. 1**: 1KB DNA Ladder used for agarose gel electrophoresis

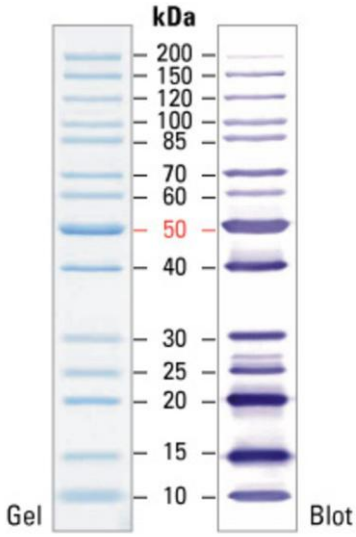



**Figure A1. 2**: PageRuler Unstained Protein Ladder for SDS-PAGE analysis

# A2 Standard Curve Data

**Table A2. 1**: Standard curve data

| ***p*-NP Conc. mM** | **Absorbance (410nm)** | **Av. Abs** |
|---|---|---|
| 0.1 | 0.029<br>0.033<br>0.036 | 0.033 |
| 0.2 | 0.068<br>0.074<br>0.076 | 0.072 |
| 0.3 | 0.104<br>0.110<br>0.110 | 0.108 |
| 0.4 | 0.132<br>0.142<br>0.142 | 0.139 |
| 0.5 | 0.178<br>0.179<br>0.197 | 0.185 |
| 0.6 | 0.197<br>0.213<br>0.205 | 0.205 |
| 0.7 | 0.219<br>0.245<br>0.237 | 0.234 |
| 0.8 | 0.241<br>0.260<br>0.258 | 0.253 |
| 0.9 | 0.280<br>0.304<br>0.310 | 0.298 |
| 1.0 | 0.367<br>0.349<br>0.392 | 0.369 |

**Table A2. 2**: Standard curve data 2, showing Standard deviation

| pNP Conc.(mM) | Abs | Abs | Abs | Average | STDEV |
|---|---|---|---|---|---|
| 0.2 | 0.068 | 0.074 | 0.076 | 0.073 | 0.003 |
| 0.4 | 0.132 | 0.142 | 0.142 | 0.139 | 0.005 |
| 0.6 | 0.197 | 0.213 | 0.205 | 0.205 | 0.007 |
| 0.8 | 0.241 | 0.260 | 0.258 | 0.253 | 0.009 |
| 1.0 | 0.367 | 0.349 | 0.392 | 0.369 | 0.018 |

# A3 NMR Spectrums

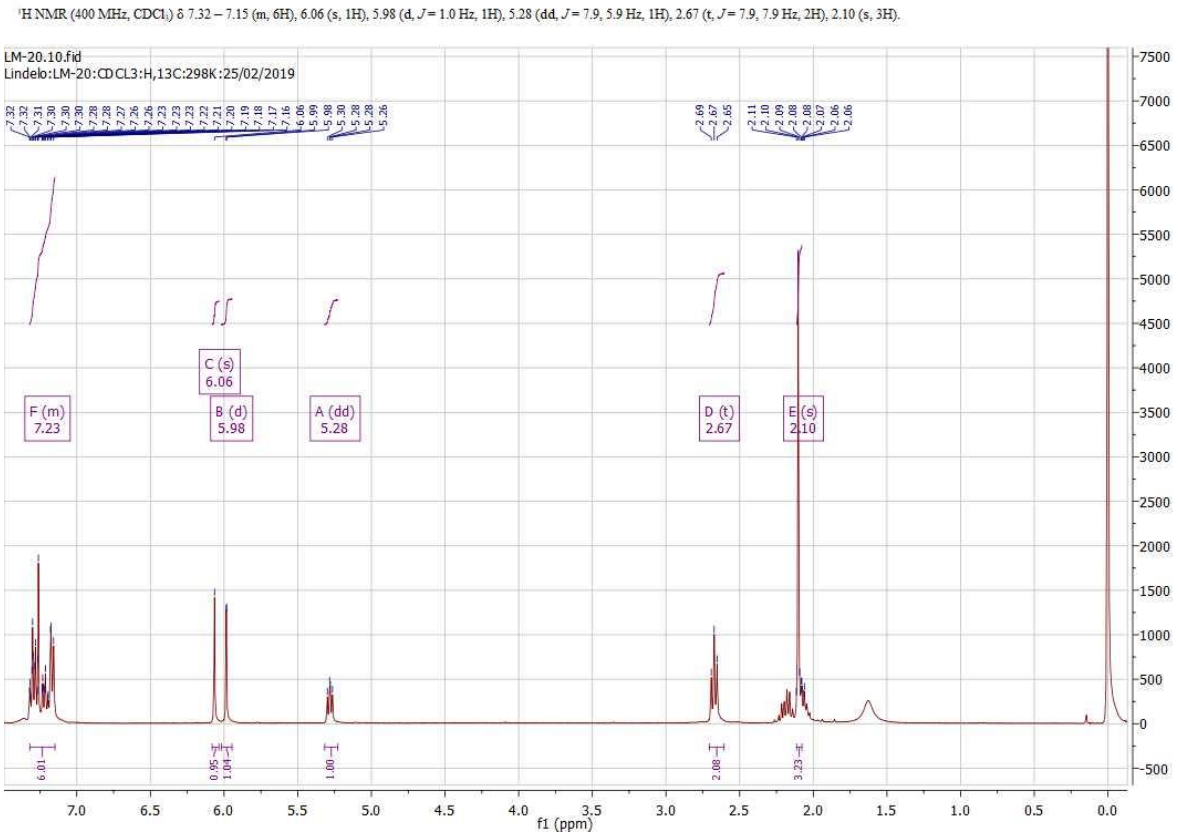



**Figure A3. 1**: $^{1}$H NMR spectra for **11a**

$^{13}$C NMR (101 MHz, $CDCl_3$) δ 169.9, 140.0, 133.0, 128.6, 128.3, 126.4, 122.6, 116.1, 72.7, 34.4, 31.2, 20.9.

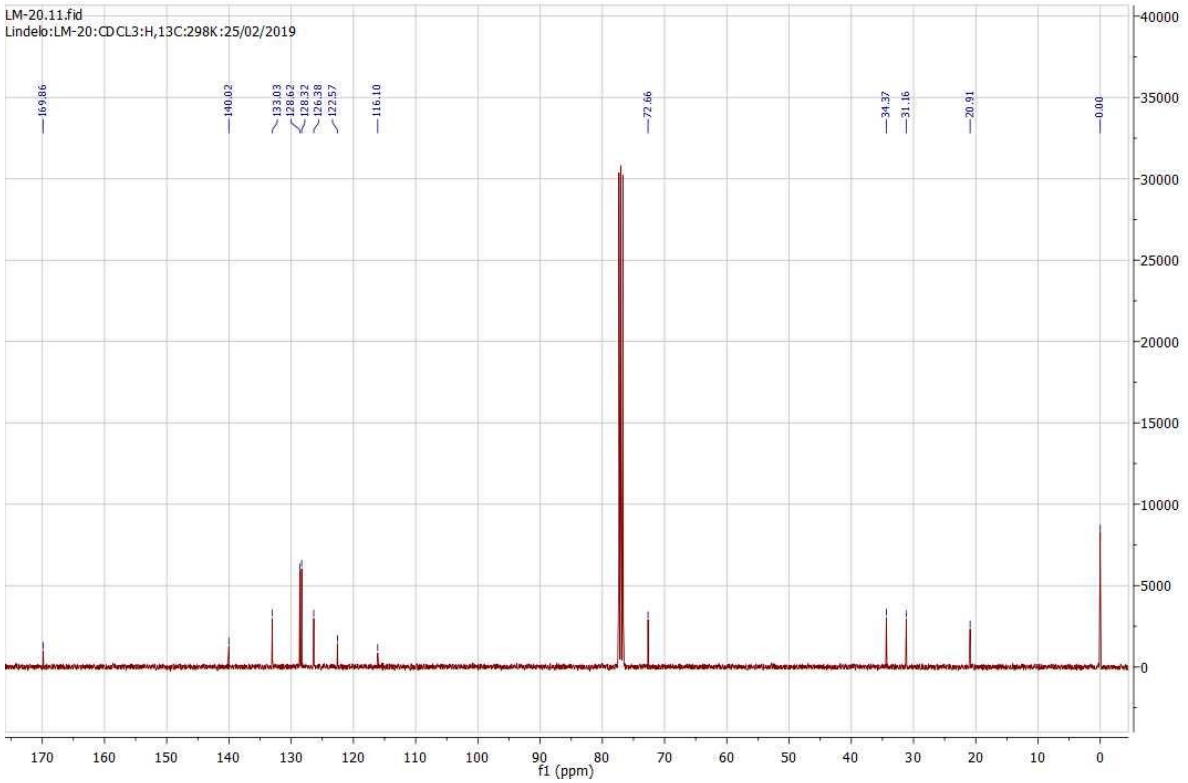



**Figure A3. 2**: $^{13}$C NMR spectra for **11a**

$^1$H NMR (400 MHz, $CDCl_3$) δ 7.40 (d, $J$ = 2.0 Hz, 5H), 6.33 (t, $J$ = 1.3, 1.3 Hz, 1H), 6.08 (d, $J$ = 1.1 Hz, 1H), 6.00 (d, $J$ = 1.3 Hz, 1H), 2.18 (d, $J$ = 1.5 Hz, 3H).

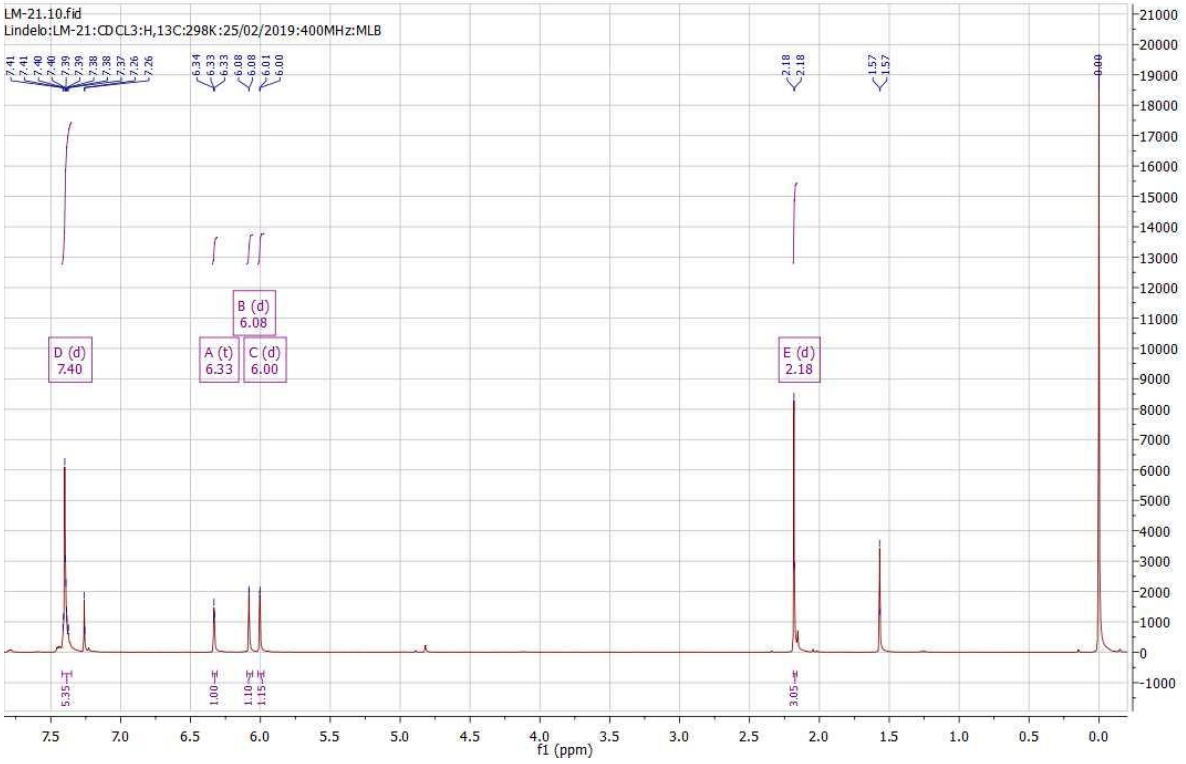



**Figure A3. 3**: $^1$H NMR spectra for **11b**

$^{13}$C NMR (101 MHz, $CDCl_3$) δ 169.3, 135.6, 132.0, 129.3, 129.2, 129.0, 127.0, 123.3, 116.2, 74.4, 21.0, 0.0.

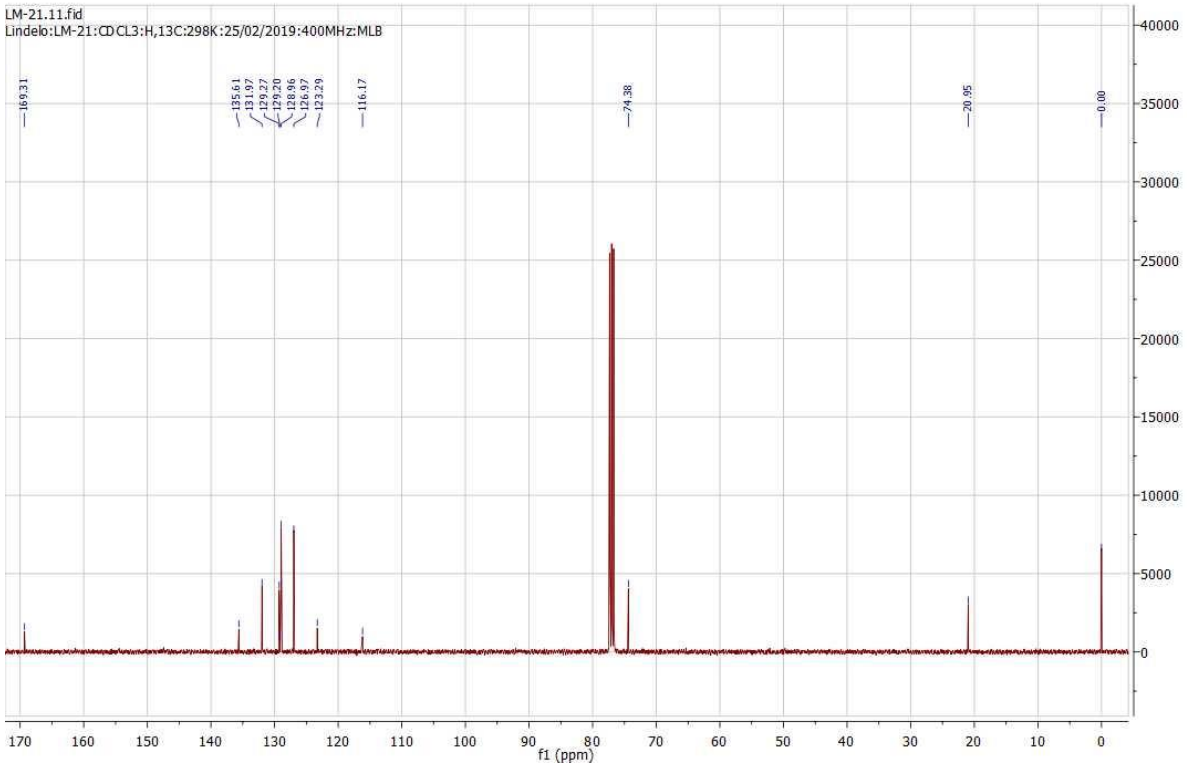



**Figure A3. 4**: $^{13}$C NMR spectra for **11b**